



RESEARCH ARTICLE

10.1002/2014GC005323

Key Points:

- New bathymetric data set for the South Orkney continental shelf
- Continental shelf extensively influenced by past glacial activity
- New glacial reconstruction for maximum glaciation

Supporting Information:

- ReadMe
- Figure S1

Correspondence to:

W. A. Dickens,
wild@bas.ac.uk

Citation:

Dickens, W. A., A. G. C. Graham, J. A. Smith, J. A. Dowdeswell, R. D. Larter, C. -D. Hillenbrand, P. N. Trathan, J. E. Arndt, and G. Kuhn (2014), A new bathymetric compilation for the South Orkney Islands, Antarctic Peninsula (49°–39°W to 64°–59°S): Insights into the glacial development of the continental shelf, *Geochem. Geophys. Geosyst.*, 15, 2494–2514, doi:10.1002/2014GC005323.

Received 4 MAR 2014

Accepted 11 MAY 2014

Accepted article online 15 MAY 2014

Published online 24 JUN 2014

A new bathymetric compilation for the South Orkney Islands region, Antarctic Peninsula (49°–39°W to 64°–59°S): Insights into the glacial development of the continental shelf

William A. Dickens^{1,2}, Alastair G. C. Graham³, James A. Smith¹, Julian A. Dowdeswell², Robert D. Larter¹, Claus-Dieter Hillenbrand¹, Phil N. Trathan¹, Jan Erik Arndt⁴, and Gerhard Kuhn⁴

¹British Antarctic Survey, Cambridge, UK, ²Scott Polar Research Institute, University of Cambridge, Cambridge, UK, ³College of Life and Environmental Sciences, University of Exeter, Exeter, UK, ⁴Alfred-Wegener-Institut Helmholtz-Zentrum für Polar- und Meeresforschung, Bremerhaven, Germany

Abstract We present a new, high resolution (300 m) bathymetric grid of the continental shelf surrounding the South Orkney Islands, northeast of the Antarctic Peninsula. The new grid, derived from a compilation of marine echo-sounding data, improves previous regional bathymetric representations and helps to visualize the morphology of the shelf in unrivalled detail. The compilation forms important baseline information for a range of scientific applications and end users including oceanographers, glacial modelers, biologists, and geologists. In particular, due to the limited understanding of glacial history in this region, the bathymetry provides the first detailed insights into past glacial regimes. The continental shelf is dominated by seven glacially eroded troughs, marking the pathways of glacial outlets that once drained a former ice cap centered on the South Orkney Islands. During previous glacial periods, grounded ice extended to the shelf edge north of the islands. A large, ~250 km long sediment depocenter, interpreted as a maximum former ice limit of one or more Cenozoic glaciations, suggests that ice was only grounded to the ~300–350 m contour in the south. Hypsometric analyses support this interpretation, indicating that a significant proportion of the shelf has been unaffected by glacial erosion. Using these observations, we propose a preliminary ice cap reconstruction for maximum glaciation of the South Orkney plateau, suggesting an ice coverage of about ~19,000 km². The timing of maximum ice extent, number of past advances and pattern of subsequent deglaciation(s) remain uncertain and will require further targeted marine geological and geophysical investigations to resolve.

1. Introduction

Advances in the accuracy, resolution, and coverage of multibeam swath bathymetry have significantly enhanced the information potential from bathymetric maps [e.g., Nitsche *et al.*, 2007; Graham *et al.*, 2008, 2011; Arndt *et al.*, 2013]. High resolution bathymetric data improve our understanding of sea floor morphology and drive advances in oceanographic, biological, geological, and glaciological research.

Specifically, our understanding of bathymetry in polar regions is crucial for the prediction of ice shelf and ice sheet responses to climate change as it: (1) controls the transfer of dense shelf water masses formed on polar shelves to the deep ocean as well as the supply of warm deep water to ice sheet grounding lines [e.g., Walker *et al.*, 2007; Thoma *et al.*, 2008; Nicholls *et al.*, 2009; Hellmer *et al.*, 2012; Pritchard *et al.*, 2012; Dutrieux *et al.*, 2014] and (2) regulates tidal dynamics and their influence on ice shelf melting and stability [e.g., Padman *et al.*, 2002; Griffiths and Peltier, 2009; Makinson *et al.*, 2011; Rosier *et al.*, 2014].

In addition, accurate bathymetry data are the key to understanding the ecology of marine flora and fauna in Antarctica and the production of habitat maps [Burns *et al.*, 2004; Flores *et al.*, 2008; Ribic *et al.*, 2008]. For example, krill concentrations, which control the distribution and breeding success of seals, penguins, and whales, are heavily influenced by bathymetry [McConnell *et al.*, 1992; Murphy *et al.*, 1997; Ribic *et al.*, 2008]. Compiled bathymetry data have also been used widely in geological studies of the Southern Ocean, with applications that range from the location and exploration of hydrothermal vent systems [Rogers *et al.*, 2012] to the detailed interpretation of volcanic arcs [Leat *et al.*, 2010].

In recent years, bathymetric grids have also been increasingly used to investigate the history of formerly glaciated regions across Antarctica [Canals *et al.*, 2002; Nitsche *et al.*, 2007; Graham *et al.*, 2008; Beaman

et al., 2011], the Arctic Ocean [Jakobsson *et al.*, 2008], and mid/high latitude regions [Ottesen *et al.*, 2005; Bradwell *et al.*, 2008]. These data sets highlight morphological features on the continental shelf that formed during periods of more extensive cover by grounded ice [e.g., Nitsche *et al.*, 2007; Graham *et al.*, 2008, 2011] which can be used, in turn, to reconstruct the characteristics of former ice sheets such as their size, extent, dynamics (e.g., velocity and basal regime), and drainage patterns. Continual improvements to bathymetric grids are particularly important to modern and palaeo-glaciological models because ice sheet growth and retreat is exceptionally sensitive to subglacial topography [Holt *et al.*, 2006; Vaughan *et al.*, 2006; Jakobsson *et al.*, 2012; Pedersen and Egholm, 2013].

The South Orkney continental shelf has been identified as a key area in which a new bathymetric grid will improve our understanding of the regional glacial history. To date, little is known about the ice caps that once dominated this microcontinent [cf. Hodgson *et al.*, 2014]. Geomorphological mapping by Sugden and Clapperton [1977], using a crude bathymetric data set based on limited spot soundings, revealed the existence of several relict glacial cross-shelf troughs. In addition, a single-channel sparker profile, collected during "Deep Freeze 1985" (DF-85), revealed a prominent unconformity extending to 240–300 m water depth [Herron and Anderson, 1990; Bentley and Anderson, 1998]; this was taken to suggest that grounded ice reached the 250–300 m isobath at some time in the past. This interpretation was also consistent with the recovery of proximal glacial/subglacial till lithofacies of unknown age in sediment cores to a depth of at least 246 m [Herron and Anderson, 1990]. Despite this early work, the size, extent, and interconnectivity of the cross-shelf troughs has remained poorly constrained due to the low resolution of available bathymetric grids. In addition, the spatially restricted distribution of seismic lines and sediment cores implies that any variations in ice cap grounding line depth across the shelf are poorly understood.

To this end, we present a new, high resolution, bathymetric grid of the South Orkney continental shelf (49°–39°W to 64°–59°S), compiling all available water depth data in order to further our understanding of shelf morphology and the glacial/geological processes that produced it. The data set will form a baseline for future palaeoglaciological investigations and provide a new data set for geological, oceanographic, and biological researchers working in this region of the Antarctic Peninsula. For the latter, this is particularly timely because the South Orkney Islands have a designated Marine Protected Area (MPA). The bathymetric data set forms the basis of a new geomorphic classification map for the South Orkney MPA (see supporting information Figure S1). The marine geomorphic zonation is a key element of habitat mapping under the CCAMLR (Commission for the Conservation of Antarctic Marine Living Resources) initiative that allows for the analysis of ecosystem properties in the region, and hence forms the basis for future marine reserve decisions [CCAMLR, 2005].

2. Geological and Oceanographic Setting

The South Orkney Islands are an archipelago centered at 60°35'S and 45°30'W, and located approximately 600 km north east of the Antarctic Peninsula (Figure 1). The broad continental shelf with an area of ~48,000 km² is the largest of the continental fragments that form the South Scotia Ridge. The South Orkney microcontinent (SOM) was separated from the Antarctic Peninsula along an E-W margin, probably during the Eocene and Early Oligocene, ~40–30 million years ago [Coren *et al.*, 1997]. The microcontinent then continued to drift and rotate until it reached its approximate modern position, relative to the Antarctic Peninsula, during the early Miocene [King and Barker, 1988; Coren *et al.*, 1997]. The absence of seismic activity within Powell Basin suggests that at present no significant relative movement between the Antarctic Peninsula and the SOM occurs [Thomas *et al.*, 2003]. The northern margin of the continental shelf coincides with a lateral (sinistral) transform margin which separates the Scotia and Antarctic plates. Earthquake focal mechanisms indicate east west strike slip motion with an element of extension [Civile *et al.*, 2012]. This conclusion is supported by recent, extraordinary seismic activity, recorded along the South Scotia Ridge, highlighting the relative motion between the two plates [Smalley *et al.*, 2013].

Oceanography in the study area is complex because it lies between the Antarctic Circumpolar Current (ACC) and the Weddell Sea Gyre. The continental shelf is bounded to the north by the southern boundary of the ACC and to the south by the Weddell Front, the northern-most extent of the Weddell Gyre. Between these two current regimes lie the waters of the Weddell-Scotia Confluence. A paucity of direct observations means we know little about the water column characteristics, though water temperatures vary between

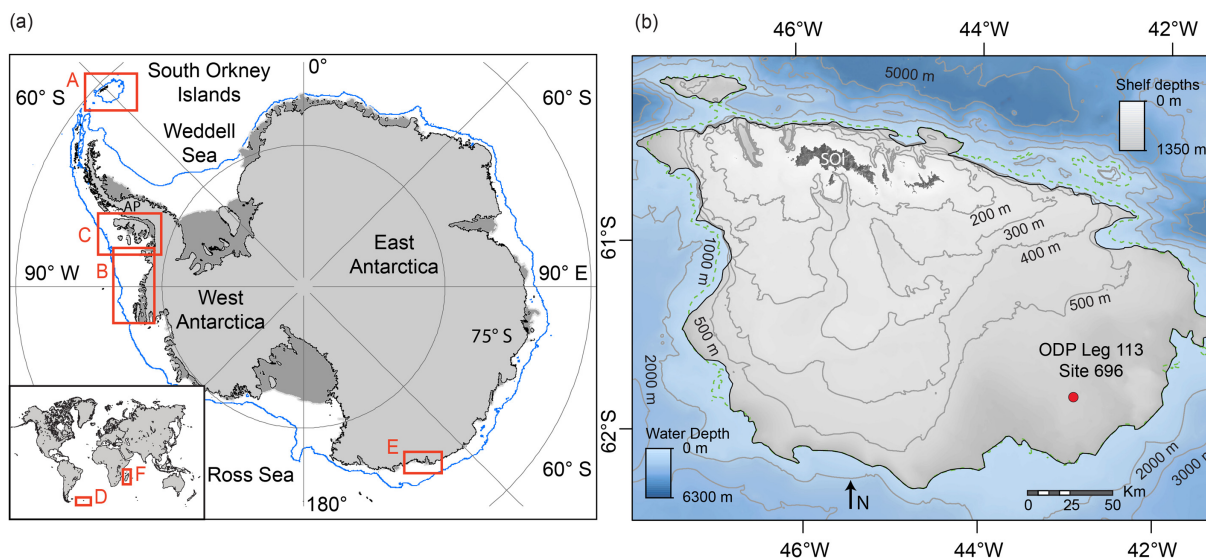


Figure 1. Location map showing (a) the location of the South Orkney Islands relative to Antarctica with the blue line delineating the shelf edge, and red boxes highlighting the location of additional bathymetric grids used for hypsometric comparison, and (b) the South Orkney microcontinent (SOI = South Orkney Islands) and the location of ODP Leg 113 Site 696. The gray-shaded areas represent the shelf edge extent and the green dashed line marks the 1000 m contour used in hypsometric analysis; this depth was chosen because it offers the best approximation of shelf edge depth across the entire region (see section 4.4.1).

−1.86° and 1.6°C at shallow depths, with significant interannual variability [Clarke and Leakey, 1996]. The islands today are characterized by a cold, maritime subpolar climate and are significantly covered by glacier ice (~85%). Meteorological observations at Orcadas Station on the South Orkney Islands, along with stations on the Antarctic Peninsula, indicate that the region has warmed significantly since the 1930's, at a rate of up to $3.7 \pm 1.6^\circ\text{C}$ a century [Vaughan *et al.*, 2003]. On and around the South Orkney Islands, this warming has been accompanied by glacier retreat [Favero-Long *et al.*, 2012] and a decrease in sea-ice [Murphy *et al.*, 1995; Meredith *et al.*, 2011].

3. Methodology

We constructed the new bathymetric grid by collating ship soundings from a number of expeditions, following the methods applied elsewhere in Antarctica [Nitsche *et al.*, 2007; Graham *et al.*, 2008; Beaman *et al.*, 2011; Graham *et al.*, 2011; Arndt *et al.*, 2013]. Unlike bathymetric compilations from further south, where significant cover by ice shelves, floating glaciers and sea ice obscures the topography, no subice data are required [e.g., Fretwell *et al.*, 2013]. This bathymetric compilation integrates newly collected multibeam swath bathymetry data from RRS James Clark Ross cruise JR244 with all other available bathymetric data from the region. This includes single-beam and multibeam data from, among others, the British Antarctic Survey (BAS) and the Alfred-Wegener-Institute (AWI), alongside additional data included within the Olex data set: a compilation of soundings compiled from fisheries industry vessels operating worldwide (Table 1 and Figure 2).

The area chosen for gridding, defined by the South Orkney continental shelf and a surrounding buffer zone, includes water depths ranging from present day sea level down to >6000 m. The extent of each data type varies considerably spatially (Figure 2) but regions close to the islands are well covered by all data types. Regions to the north and west of the shelf have an extensive coverage of all data types, although coverage on the southwestern shelf edge is irregular and discontinuous. In addition, the southern and southeastern regions, both inner and outer shelf, have a much sparser coverage, relying largely on single-beam data; this is reflected in the final product—a sparse data set will result in more heavily interpolated bathymetry which will appear smoother with less surficial detail. There is also more limited data coverage directly north of the islands (Figure 2).

3.1. Pregridding Steps

The processing steps used to produce this bathymetric grid are shown in Figure 3. We gridded multibeam data from 48 cruises between 1986 and 2012 at a 50 m resolution using MB-system [Caress and Chayes, 1996]. The vertical accuracy of multibeam data is usually better than 0.2% of water depth,

Table 1. Data Sets Used in the South Orkney Compilation^a

Survey Type	Survey ID	Year	Source	Survey ID	Year	Source	
MBES	JR66	2001	BAS	JR280	2012	BAS	
	JR71	2002	BAS	ANT-IV/4	1986	AWI	
	JR77–78	2004	BAS	ANT-V/4	1986	AWI	
	JR97	2005	BAS	ANT-VI/3	1987	AWI	
	JR109	2004	BAS	ANT-VIII/5	1989	AWI	
	JR114	2005	BAS	ANT-X/5	1992	AWI	
	JR130	2004	BAS	ANT-XII/3	1995	AWI	
	JR134	2005	BAS	ANT-XV/2	1997	AWI	
	JR149	2006	BAS	ANT-XV/4	1998	AWI	
	JR151	2005	BAS	ANT-XIX/5	2002	AWI	
	JR184	2007	BAS	ANT-XXII/2	2004	AWI	
	JR185	2007	BAS	ANT-XXII/3	2005	AWI	
	JR187	2008	BAS	ANT-XXII/4	2005	AWI	
	JR188	2008	BAS	ANT-XXIII/7	2006	AWI	
	JR228	2009	BAS	ANT-XXVII/3	2011	AWI	
	JR239	2010	BAS	GAP95	1995	AWI	
	JR244	2011	BAS	GAP98	1998	AWI	
	JR252	2011	BAS	Hes97	1996	IACT	
	JR254–264-265	2011	BAS	Hesant923	1992	IACT	
	JR257	2012	BAS	HMOI1190	2007	BAS/UKHO	
	JR259	2012	BAS	HMOI1198	2007	BAS/UKHO	
	JR262	2011	BAS	NBP0805	2008	LDEO MGDS	
	JR275	2012	BAS	NBP9705	1997	LDEO MGDS	
	JR279	2012	BAS	NBP1105	2011	LDEO MGDS	
	SBES	19920020	1989	BAS	End_778	1977	BAS
		19920136	1991	BAS	EShack00	2000	BAS
19920140		1992	BAS/UKHO	EShack01	2001	BAS	
19930046		1983	BAS	EShack02	2002	BAS	
19940038		1994	BAS	EShack99	1999	BAS	
19950340		1987	BAS/UKHO	i0876	1976	NGDC	
19950342		1987	BAS	IR193–94	1993	AA	
19950342		1987	BAS/UKHO	JR01	1992	BAS	
19950348		1995	BAS/UKHO	JR04	1993	BAS	
19960009		1985	BAS	JR06 (Leg2)	1994	BAS	
19970238		1997	BAS/UKHO	JR09b	1995	BAS	
A19495		1994	NGDC	JR10	1995	BAS	
ANTIV/4		1986	AWI	JR18	1997	BAS	
ANTVI/3		1987	AWI	JR39a	1999	BAS	
Bisc_867		1987	BAS	JR47	2000	BAS	
Bran_745		1975	BAS	L1578	1978	NGDC	
Bran_756		1976	BAS	Mma_867	1986	ODP	
Bran_767		1976	BAS	NBP93-1	1993	NGDC	
Bran_778		1977	BAS	ODP113J	1987	ODP	
Bran_789		1978	BAS	PROTO4MV	1983	Scripps/NGDC	
Bran_790		1980	BAS	Shack_68	1968	BAS	
CD37_889		1989	BAS	Shack_71	1971	BAS	
D154_845		1984	BAS	Shack_73	1973	BAS	
D172_878		1987	BAS	Shack_75	1975	BAS	
DF85		1985	NSF/NGDC	Shack_80	1980	BAS	
ELT22		1965	NGDC	Tha81	1981	NGDC	
End_690		1969	BAS	VLCN06MV	1981	Scripps/NGDC	

^aMBES = Multibeam echo sounder, SBES = Single-beam echo sounder. BAS = British Antarctic Survey, UKHO = UK Hydrographic Office, NSF = National Science Foundation, NGDC = National Geophysical Data Centre, AWI = Alfred Wegener Institute, IACT = Instituto Andaluz de Ciencias de la Tierra, LDEO MGDS = Lamont-Doherty Earth Observatory Marine Geoscience Data System, AA = Armada Argentina, ODP = Ocean Drilling Program.

though this can increase in regions of steep topography. Horizontal positioning data were not reexamined as the accuracy and precision is an order of magnitude better than the final resolution of the data. Multi-beam data sets were already processed and calibrated using sound velocity profiles (SVPs) from respective cruises. We assessed their accuracy by examining the gridded data sets individually; data sets showed “flat” bathymetry across-track, as expected for good sound velocity control, and depths were found to correspond well in areas of data overlap. In certain locations, i.e., the southwest plateau, the quality of multibeam data appears patchy and discontinuous (Figure 2). This can be caused by the use of high frequency systems in deep water or it may reflect data artifacts resulting from, among other factors, sea ice.

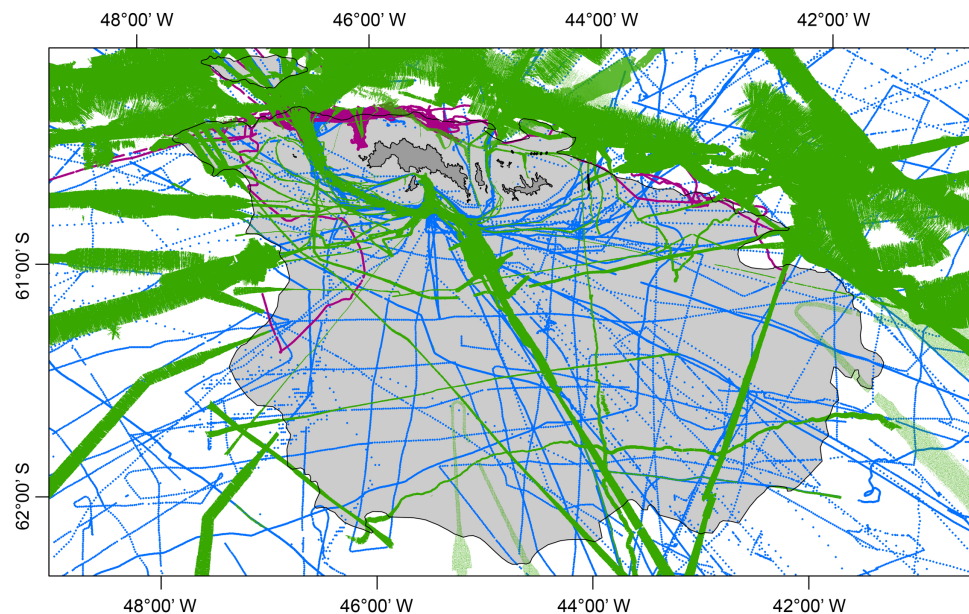


Figure 2. The spatial extent of contributing data (shelf area highlighted) to the bathymetric compilation. Single-beam data are shown with blue lines, multibeam data are shaded in green, and Olex data are shaded in pink.

Typically, the data were already processed but some required additional cleaning to remove erroneous points; this was performed using Fledermaus IVS [Mayer *et al.*, 2000] and the CUBE algorithm (Combined Uncertainty and Bathymetric Estimator). Once cleaned, multibeam swath bathymetry data were imported into ArcGIS (ESRI) and subsequently converted to points for gridding. Single-beam data and Olex fisheries (single-beam) data were also incorporated into the new bathymetry. Single-beam data typically has a vertical accuracy better than 1% of water depth, but this is likely to vary between surveys. Both data sets were imported directly into ArcGIS (cleaning was performed as an iterative process during the gridding procedure, see section 3.2). An ASTER DEM (ASTER GDEM is a product of METI and NASA) of the South Orkney Islands was incorporated to represent the terrestrial relief.

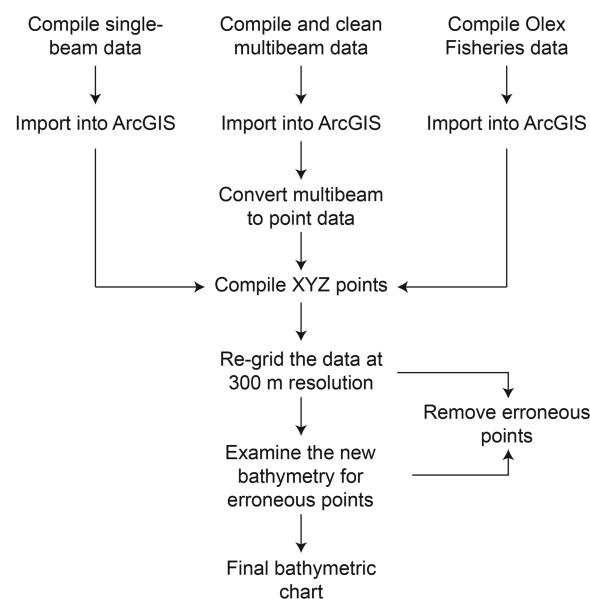


Figure 3. The processing steps followed in the production of this bathymetric compilation.

3.2. Gridding Process

Following other similar compilations (e.g., Bedmap 2) [Fretwell *et al.*, 2013], “TOPO-GRID” was used to grid the final bathymetry as it proved the most effective at incorporating spatially discontinuous data sets with various resolution and density.

TOPOGRID is built on ANUDEM, a powerful and efficient, locally adaptive interpolation program designed to work with multiple data types (e.g., contour, point data, etc.) [Hutchinson, 1988, 1989; Hutchinson *et al.*, 2011]. ANUDEM produces an interpolated grid at varying scales that is able to retain small features such as ridges and channels [Hutchinson, 1988, 1989].

TOPOGRID reads each data point and trims the coverage to a user-defined extent, in this case 49°–39°W to 64°–59°S. The algorithm averages out the

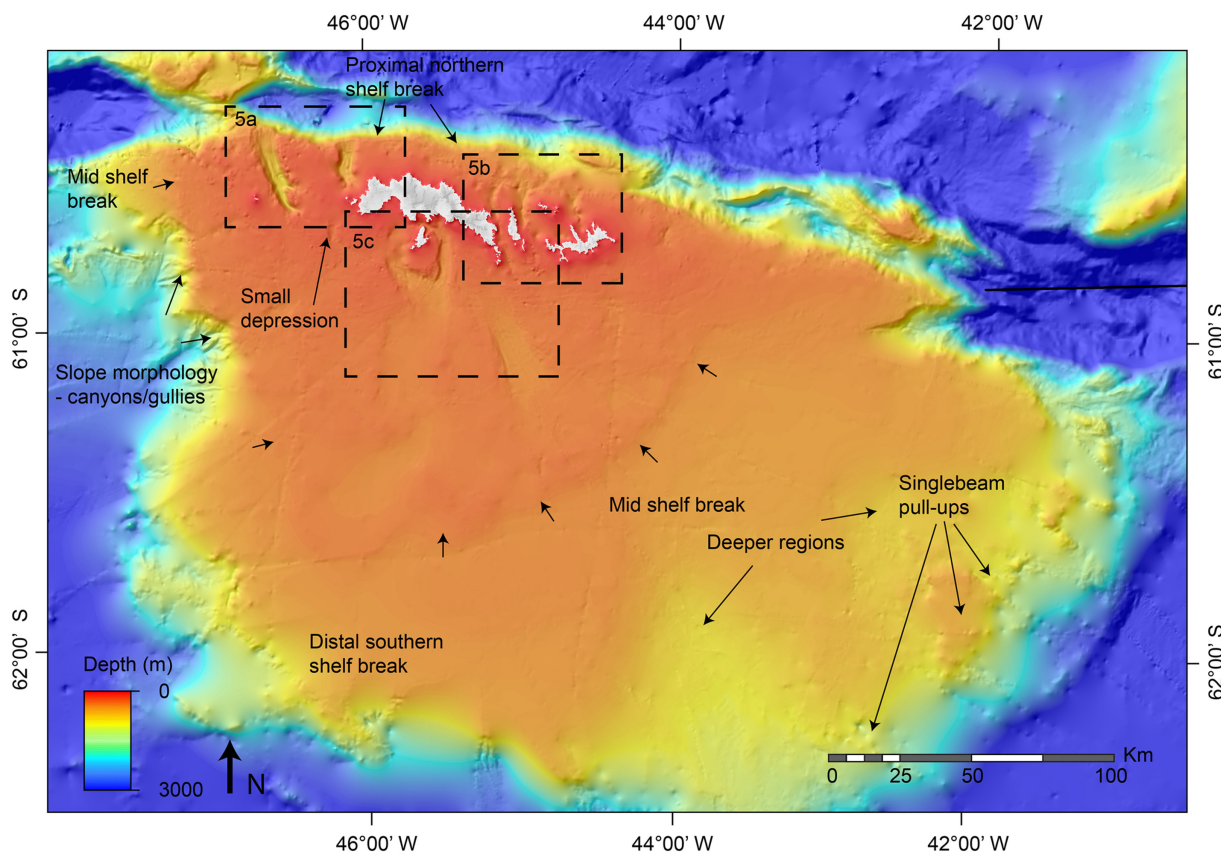


Figure 4. New bathymetric compilation for the South Orkney Islands. The hashed boxes delineate the regions used to compare this bathymetric grid with previous grids (Figure 5). The full bathymetric grid is available online; see the acknowledgements.

elevation data on to a coarse resolution grid which undergoes multiple, iterative, interpolation cycles; successively finer resolution grids are produced until the user defined resolution is obtained. After each iteration, the grid values are calculated using the Gauss-Seidel iteration with over relaxation method ([Hutchinson *et al.*, 2011]; see Hutchinson [1989] for a detailed description of the interpolation procedure). The quality of data varied between surveys, affected by a number of factors including the use of inappropriate sound velocity profiles, variable degrees of data cleaning or acquisition artifacts. The latter often results in the presence of “sinks” and “peaks”, artifacts that artificially drag up or pull down the surrounding bathymetry. A number of iterations were thus required to remove disparate points from the point cloud; these were manually removed using the Editor toolbox in ArcGIS.

The new bathymetric grid is projected in UTM (Universal Transverse Mercator) zone 23S and has a spatial resolution of 300 m—this is high enough to preserve the quality of new multibeam data while achieving a compromise with the lower resolution data sources.

3.3. Accuracy

The development of the grid utilized ~75 million points, 98% of which are from multibeam sources. However, this value decreases notably toward the south and east of the grid. Uncertainty in the new compilation was evaluated by comparing a subset of input values (1000 points) against the corresponding values in the new bathymetry. In regions where multibeam bathymetry data are present, the new bathymetry has a vertical RMS error of 29 m and a Mean Absolute Error of 15 m. In regions where single-beam data dominate, vertical RMS error increases to 154 m while the Mean Absolute Error increases to 32 m. The discrepancy reflects the sparse coverage of single-beam data, which also include some individual erroneous points that have a significant impact on the overall accuracy.

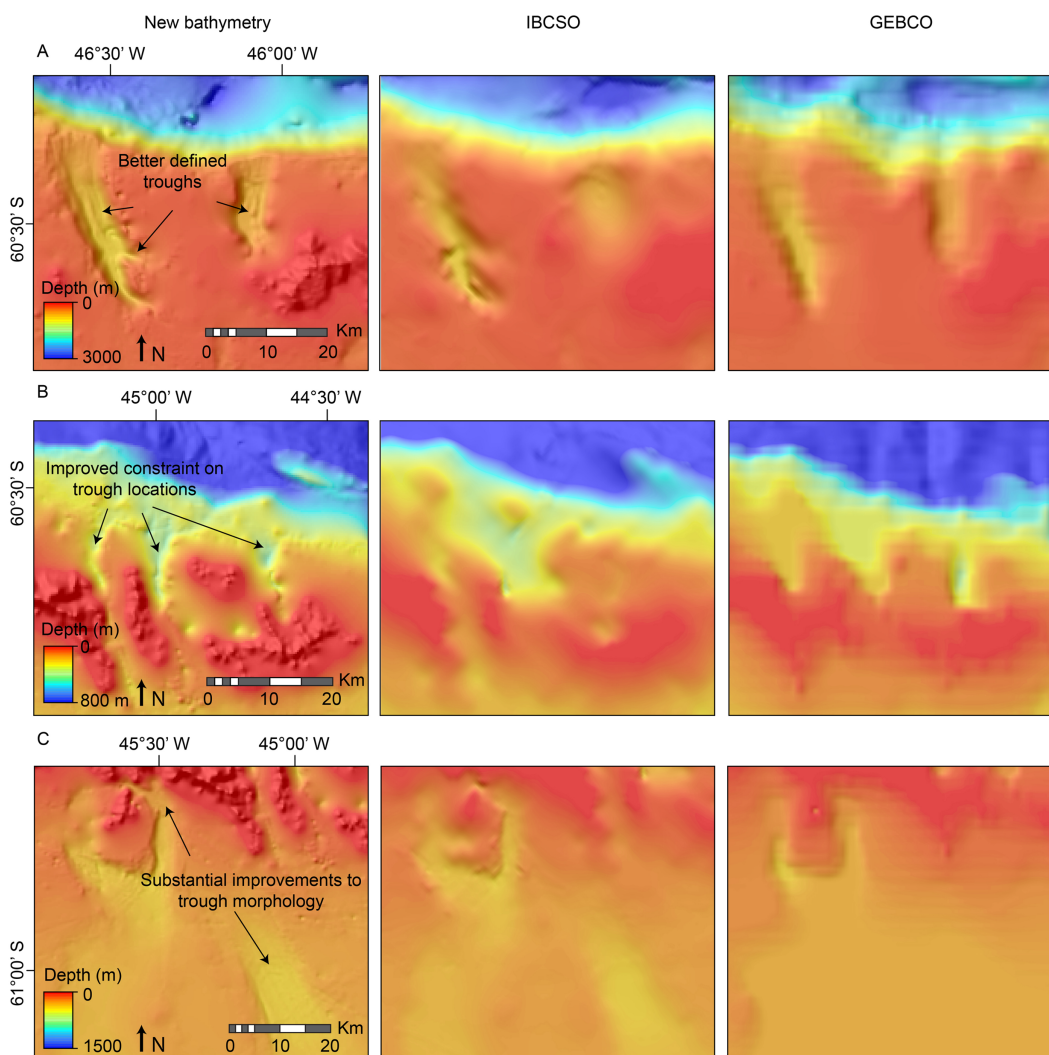


Figure 5. A comparison of the new bathymetric grid against IBCSO [Arndt *et al.*, 2013] and GEBCO [GEBCO, 2008], highlighting the improvements. The comparisons are from (a) the northwest shelf, (b) north of the islands, and (c) the southern troughs; locations for these regions are displayed in Figure 4.

4. Results and Interpretation

4.1. Regional Morphology

The new bathymetric grid (Figure 4) covers $\sim 330,000 \text{ km}^2$ and offers significant improvements over previous bathymetric representations of the continental shelf (Figure 5). The new data set reveals:

1. A deeper and more extensive set of troughs north-west of the islands, with a significant advance in the delimitation of trough margins and tributaries (Figure 5a).
2. A better constrained imaging of troughs north east and south of the islands (Figures 5b and 5c), with a considerable revision in extent compared to the recent International Bathymetric Chart of the Southern Ocean (IBCSO) compilation [Arndt *et al.*, 2013] (Figure 5).
3. A much sharper shelf edge and steeper continental slope north of the islands, and a better resolved series of morphological features on the northern and western continental slopes (Figure 4).
4. A shelf/plateau-wide mid-shelf break with a relief of $\sim 100 \text{ m}$, which separates an upper and lower shelf plateau (Figures 4 and 8).

Measured linearly from north to south and east to west (at the most distal locations) the South Orkney continental shelf is $\sim 210 \text{ km}$ long and $\sim 315 \text{ km}$ wide. The South Orkney Islands sit toward the north of this

broad, almost circular, continental shelf which has a significantly larger surface area ($\sim 48,000 \text{ km}^2$ above the shelf edge) than the modern land area (620 km^2). North of the islands, the continental shelf deepens gradually ($\sim 1.0\text{--}2.0^\circ$) to the shelf edge, which lies between 10 and 30 km from the modern coastline. The continental slope is extremely steep, around $10^\circ\text{--}18^\circ$ and greater than 20° in places, and water depths increase rapidly to $>5000 \text{ m}$.

South of the islands, the seaward dip of the shelf is much more gradual. The bathymetry generally deepens at an angle of $\sim 0.1\text{--}0.5^\circ$ —an order of magnitude lower than the northern shelf—and the shelf edge is more distal, between 65 and 200 km from the islands, resulting in a broader shelf profile that gradually rolls into deeper waters. Toward the south and east, the shelf gradient is steeper, descending to two large areas of deeper shelf (Figure 4). The continental slope, with a gradient of $\sim 2.5^\circ\text{--}8^\circ$, is considerably less steep south of the block than in the north and maximum water depths further offshore are shallower ($>3000 \text{ m}$).

4.2. Trough Systems

The South Orkney shelf is dominated by a series of deeply incised ($\sim 400\text{--}800 \text{ m}$ water depth) cross-shelf troughs which extend outward from the South Orkney Islands (Figures 4 and 6). The distribution of troughs is broadly consistent with those identified by *Sugden and Clapperton* [1977] although the new data set allows the trough morphology to be mapped and described in significantly greater detail.

4.2.1. Description

Four troughs which are eroded into the shelf have been identified on the new bathymetry, two of which discharge to the south of the islands (Figure 6) and two to the north. All systems exhibit characteristics typical of glacially carved Antarctic cross-shelf troughs, with troughs converging on the inner parts of the shelf and shallowing seaward [e.g., *Ó Cofaigh et al.*, 2005a; *Graham and Smith*, 2012; *Larter et al.*, 2012; *Livingstone et al.*, 2012]. At least three additional troughs exist in the north central part of the shelf (Figure 6) but, due to sparse multibeam coverage, it is difficult to assign values to their size, extent or connectivity. In addition, a small depression is present to the west of Signy Trough (Figure 4) although this feature is small and poorly resolved, and therefore, has been left unnamed. No troughs have been identified directly north of the islands but a low density of depth soundings in this region (Figure 2) means they may not be represented in the bathymetry. The pattern of troughs appears to be radial from the coastline which is typical of other subpolar plateaus (e.g., South Georgia, [*Graham et al.*, 2008]). In the following, the characteristics of the main troughs are outlined in more detail.

Monroe and Coronation Troughs: The two northern troughs, referred to herein as Monroe Trough and Coronation Trough (Figure 6), are orientated NNW and N, reaching maximum water depths of ~ 800 and 600 m , respectively (Table 2). Cross profiles reveal U-shaped, steep sided valleys with flat bottoms (Figure 6). Both systems have well-defined onset zones and extend to the shelf edge with lengths of 32 and 16 km, respectively. The troughs are narrowest on the inner shelf but show little variation once maximum width is reached on the mid to outer shelf ($\sim 10 \text{ km}$ for Monroe Trough and 8 km for Coronation Trough). Long axis profiles (Figure 6) reveal a rapidly seaward deepening sea floor in the onset of Monroe Trough, whereas the floor of Coronation Trough exhibits a much gentler slope. Both troughs display the seaward shallowing typical of Antarctic glacial troughs that have been shaped by inner shelf glacial erosion, outer shelf deposition, and outer margin flexure due to ice loading [*Graham and Smith*, 2012; *Larter et al.*, 2012].

In contrast to many West Antarctic (palaeo-)ice stream troughs that continue to deepen beneath the modern ice sheet grounding line, South Orkney troughs have clear onset zones. The onsets of Monroe and Coronation Troughs occur ~ 18 and 5 km , respectively, from the modern coastline. Unlike Coronation Trough, Monroe Trough extends offshore from at least two small tributaries (Figure 6). Both tributaries are between 2 and 4 km in width and deepen rapidly into the deeper and wider main trough.

Signy and Orwell Troughs: Significant morphological differences exist between Monroe and Coronation Trough to the north, and the two trough systems to the south, herein referred to as Signy and Orwell (Figure 6). Signy and Orwell Troughs are orientated SSW and SSE, respectively, and shallower than their northern counterparts, reaching maximum water depths of $\sim 400 \text{ m}$. Cross profiles show broadly U shaped, flat bottomed valleys with side walls that are less steep than in the northern troughs, particularly in the case of Signy Trough (Figure 6). Lengths of Signy and Orwell troughs are significantly greater than those in the north, being 125 and 57 km, respectively.

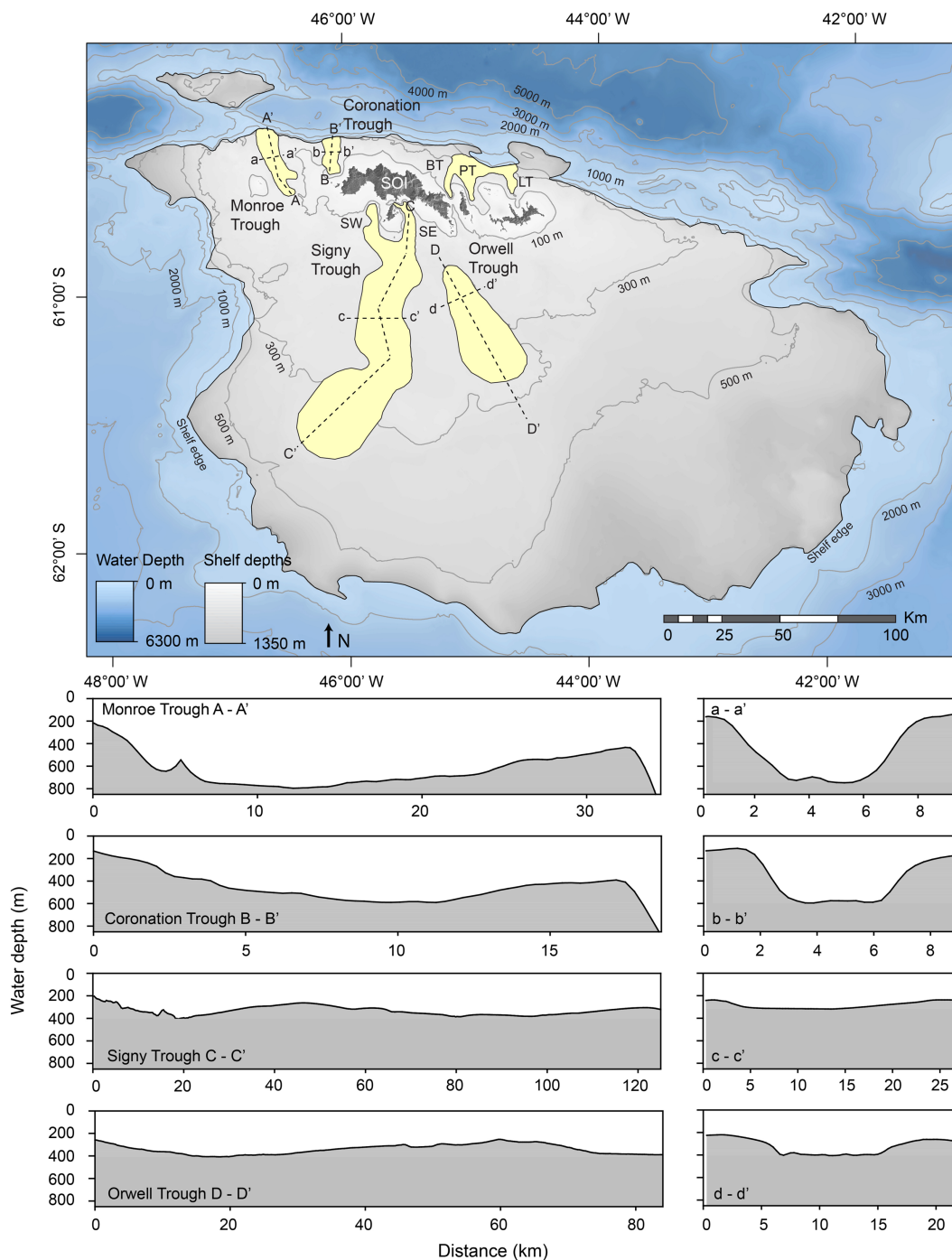


Figure 6. The new bathymetric compilation, shaded to accentuate the shelf area above the shelf edge and the trough systems (shaded in yellow). Contours on the shelf are 100, 300, 500, and 1000 m. Contours on the slope and basin are 2000, 3000, 4000, and 5000 m water depth. BT = Bennett Trough, PT = Powell Trough, LT = Laurie Trough, SW = Signy West, SE = Signy East. Locations for the cross and long trough profiles in the bottom four panels are marked on the map.

Signy Trough has two tributaries, named here as Signy East and Signy West (4–7 km in width), which merge south of Signy Island into Signy Trough (up to 30 km wide in places); both tributaries initiate close to the modern coastline. Signy Trough exhibits an irregular morphology: width varies greatly along its length, narrowing at two locations, and the long axis meanders repeatedly. In addition, trough depths shallow significantly 40 km along the trough from its northern end, before deepening again further south (Figure 6). The

Table 2. Key Morphological Characteristics of the South Orkney Troughs

Trough Name	Length (km)	Width (km)	Max Depth (km)	Area (km ²)	Tributaries
Monroe	32	10	0.8	232	2
Coronation	16	8	0.6	106	0
Signy	125	30	0.4	2538	2
Orwell	57	25	0.4	990	0
Powell ^a	20	4.5	0.4	–	0
Laurie ^a	13	4.5	0.45	–	0
Bennett ^a	20	3	0.34	–	0

^aApproximate measurements.

deepening farther offshore is more subtle but extends for a greater distance. Orwell Trough widens and shallows seaward but, unlike Signy Trough, has no tributaries and its head lies ~20 km from the coastline.

Powell, Laurie, and Bennett Troughs: Detailed examination of the new grid (Figure 7) reveals three additional elongated depressions to a maximum water depth of ~450 m

just north of Powell and Laurie Islands; these small N-S orientated troughs are herein referred to as Powell, Laurie and Bennett Troughs (Figures 6 and 7). Two small depressions close to Laurie Island (Figure 7) suggest that the head of Powell Trough might actually occur closer inland with the trough axis being located to the south of the Saddle and Weddell Islands, although the new bathymetry does not fully resolve the extent of these features. All three of these troughs widen significantly (~2–3 km wide on the inner shelf) toward the shelf edge and appear to coalesce into a large ~30 km wide and generally <400 m deep depression which extends up to, or close to, the shelf edge.

4.2.2. Interpretation

On the basis of their cross and long profiles, cross-shelf alignment and distinctive morphology, combined with the presence of subtle bedforms in several of the troughs (e.g., a smoothed linear ridge along the central axis of Monroe Trough), the cross-shelf troughs probably reflect the erosional signature of well-established, large-scale drainage outlets from a former ice cap centered around the South Orkney Islands. Similar troughs have been identified across Antarctica [Canals et al., 2002; Evans et al., 2005; Graham et al., 2011; Graham and Smith, 2012; Larter et al., 2012; Livingstone et al., 2012], the sub-Antarctic [Graham et al., 2008], and the northern hemisphere [Ottesen et al., 2005; Ó Cofaigh et al., 2013]. The troughs would have focused ice flow and acted as pathways for ice drainage, as in ice-stream troughs in the modern polar ice sheets. Despite the lack of multibeam coverage on the north eastern shelf, it seems likely that Powell, Laurie, and Bennett Troughs are also former glacial outlets.

The inter-trough areas are significantly shallower and exhibit little variation in slope, dipping fairly continuously to the shelf edge. While the troughs focused ice flow, the intervening banks may have supported

slow moving ice; a feature typical of Antarctic and Arctic shelf glaciations [Dowdeswell and Elverhoi, 2002; Ottesen et al., 2005; Ottesen and Dowdeswell, 2009; Klages et al., 2013].

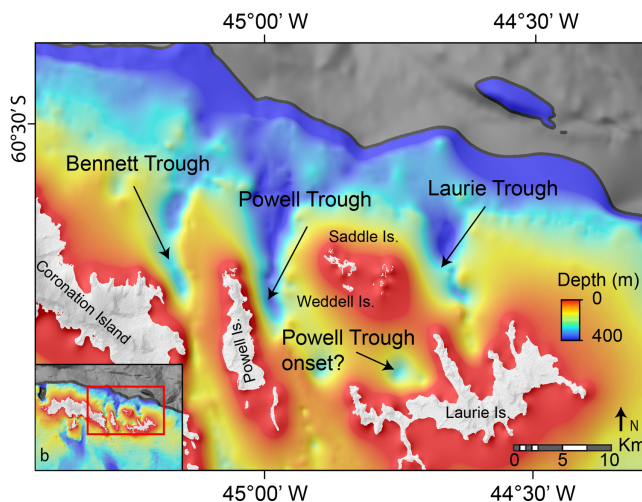


Figure 7. Bennett, Powell, and Laurie Troughs, displayed with an exaggerated depth scale, 0–400 m water depth. The gray regions are sea floor >550 m water depth (an approximation of the shelf edge in this region). Inset (b) shows the setting of these trough systems.

4.3. Mid-shelf Break
4.3.1. Description

Together with the well-developed troughs, the most prominent shelf feature from the new bathymetric compilation is a large mid-shelf break in slope which is orientated parallel to the shelf edge (Figures 4 and 8). The break has >100 m relief along most of its length and separates what can be broadly defined as an upper and lower shelf plateau (Figures 4 and 8). The trough systems are limited to, and dominate,

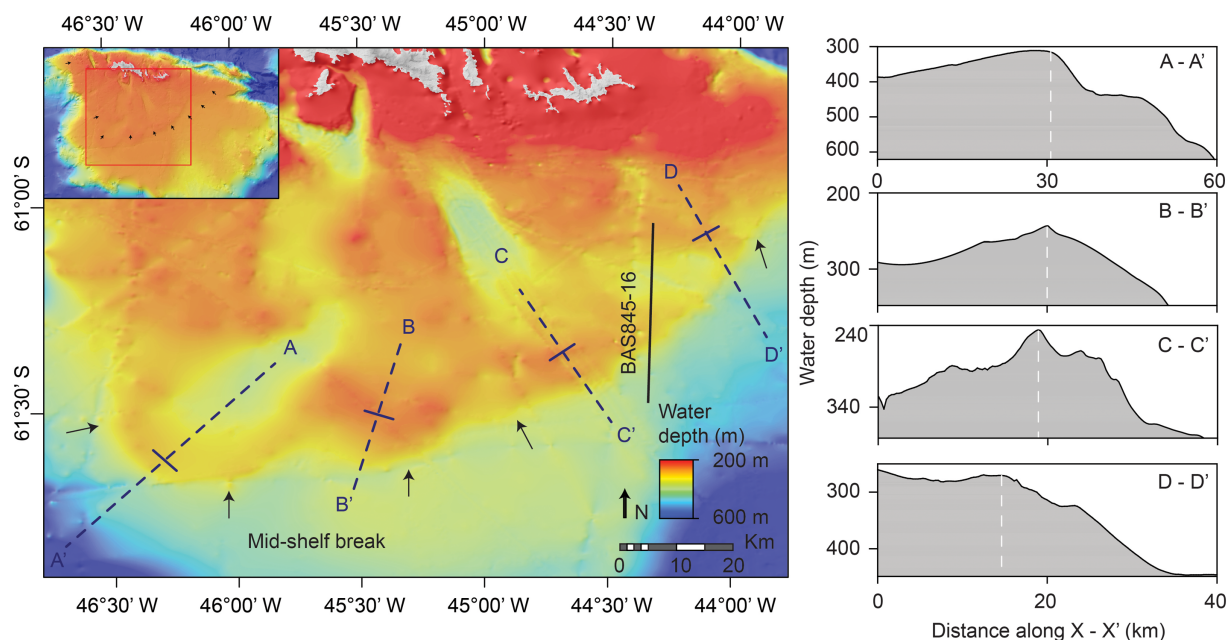


Figure 8. The mid-shelf break, displayed with an exaggerated color bar scale (200–600 m water depth). The location of the profiles is displayed on the map. The horizontal line across each profile location corresponds with the gray-hashed vertical line on each profile (these are designed to show the varying position of the mid-shelf break). The image also highlights the raised sediment wedges close to the mid-shelf break. Inset figure highlights the setting of this mid-shelf break.

the upper plateau, while the lower plateau shows little morphological variation, with water depths increasing gradually to the shelf edge. The mid-shelf break is best developed on the central, southern shelf but is absent north of the islands; in these regions the upper plateau extends to the shelf edge.

Bathymetric profiles across the mid-shelf break (Figure 8) reveal a wedge-like morphology, with amplitudes of ~ 10 – 30 m, widths of >6 – 15 km (perpendicular to the shelf edge) and a relief of >100 m on the seaward flank. While profiles vary along the break, with slope gradients that typically range from 0.5° to 1.2° , an asymmetric form is particularly pronounced in the SW of the shelf (profile A in Figure 8). Two of the largest wedges (Figure 8, profiles A-A' and C-C') are situated at or close to the southern limits of Signy and Orwell Troughs. In addition, the break exhibits a distinct lobate form around the mouth of Signy Trough and a shallow bank to its east, with a less arcuate shape around the mouth of Orwell Trough. The overall size and scale is similar in form to features found on formerly glaciated shelves across Antarctica and the Arctic [Ottesen *et al.*, 2007; Graham *et al.*, 2008; Dowdeswell and Fugelli, 2012; Dowdeswell and Vasquez, 2013].

Multichannel Seismic line BAS845-16 (Figure 9; see Figure 8 for location) reveals the internal structure of the mid-shelf break. Despite the relatively low resolution of the seismic data, which were acquired to study the crustal structure of the South Orkney microcontinent during RRS Discovery cruise D154, the mid-shelf feature appears to overlie a sequence of conformable, stacked acoustic reflectors. We interpret these stratified seismic units as sedimentary strata. They clearly extend underneath the mid-shelf break inshore of the break, and beyond the feature toward the outer South Orkney plateau. Thus, the seismic data clearly illustrate that the mid-shelf break identified in our bathymetry grid is a depositional feature rather than of tectonic origin.

4.3.2. Interpretation

Based on the distinctive geometry, sedimentary composition, association with glacial troughs that terminate at the mid-shelf break and the similarities to glacial deposits observed elsewhere, the large mid-shelf break is interpreted as a plateau-wide glacial sedimentary depocenter which formed at the terminus of one or more grounded ice caps. The internal seismic stratigraphy of the feature (Figure 9), although poorly resolved, is more chaotic in nature than the lower stratified units, consistent with the interpretation of the feature as a glacial depocenter comprising diamicton-dominated glacial sediments [Stewart and Stoker, 1990]. Furthermore, the absence of erosional unconformities or chaotic seismic units seaward of the

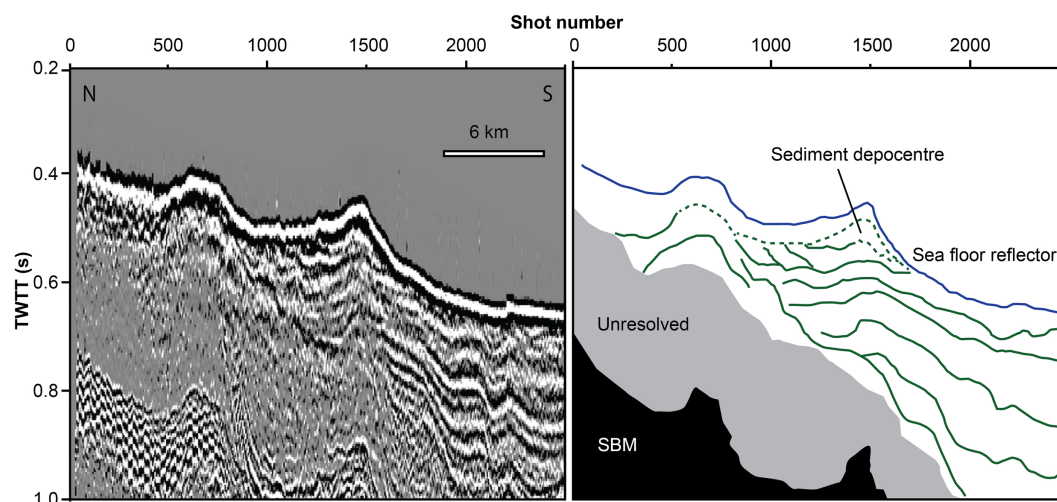


Figure 9. Seismic line BAS845-16 and corresponding interpretation, the location of which is displayed in Figure 8. SBM = Sea bottom multiple.

mid-shelf break suggests that it probably marks the limit of glaciogenic sediment delivery during late Quaternary glacial cycles.

4.4. Hypsometry

To better understand the morphology of the South Orkney Islands and the surrounding continental shelf, hypsometric analysis was performed on the new bathymetric compilation. Hypsometry examines the distribution of area relative to elevation. Insights from numerical models, sediment yields and morphological differences between glacial and fluvial valleys all attest that wet-based glacial systems have a greater erosional efficacy than fluvial systems [Brocklehurst and Whipple, 2002; Montgomery, 2002; Spotila *et al.*, 2004; Dowdeswell *et al.*, 2010]. As a result, glaciated landscapes show distinct hypsometric distributions that provide clues to their long-term morphological development and the dominant landscape modifiers [Brocklehurst and Whipple, 2002; Egholm *et al.*, 2009; Pedersen and Egholm, 2013].

4.4.1. Description

Hypsometric analysis was performed on the South Orkney shelf, using the 1000 m contour as an approximation of the shelf edge. This ensured that biases were not introduced into the analysis in regions where a low multibeam coverage meant the shelf edge was uncertain. The results reveal a limited surface area at shallow water depths with <12% ($\sim 5900 \text{ km}^2$) above the 200 m bathymetric contour (Figure 10a). Instead, surface area is concentrated between ~ 200 and 500 m water depth; more than 53% ($\sim 26,200 \text{ km}^2$) lies within this range. Although surface area is greatest at mid depths, distribution of the remaining $\sim 35\%$ ($\sim 16,900 \text{ km}^2$) is relatively even across the subsequent intervals. It is only below water depths of 900 m that surface area within each depth interval decreases notably. This concentration of surface area at mid depths, and the minimal surface area at shallow depths, produces a distinct hypsometric curve (Figure 10a). At shallow depths the curve exhibits a concave upward profile, with the curve gradually becoming convex upward as water depth increases.

4.4.2. Interpretation

The hypsometric curve for the South Orkney continental shelf is similar in form to hypsometric curves derived from bathymetric compilations of equivalent resolution from the Bellingshausen and Amundsen Seas, South Georgia and Terre Adélie Land (Figures 10b–10e) [Nitsche *et al.*, 2007; Graham *et al.*, 2008; Beaman *et al.*, 2011; Graham *et al.*, 2011]. These Antarctic shelves are all known to have an extensive glacial history [McMullen *et al.*, 2006; Nitsche *et al.*, 2007; Graham *et al.*, 2008, 2010; Hillenbrand *et al.*, 2010; Beaman *et al.*, 2011; Smith *et al.*, 2011; Graham and Smith, 2012], with numerous shelf edge glaciations throughout the Quaternary and earlier times. Similar profiles have also been observed for formerly glaciated shelves in the Arctic [Emery, 1979; Jakobsson, 2002]. In addition, Emery [1979] noted that the formerly glaciated basins all had greater mean and median depths than non-glaciated regions. In contrast, hypsometry from Madagascar, a non-glaciated shelf, reveals a continuous convex upward profile. Jakobsson [2002] also noted that

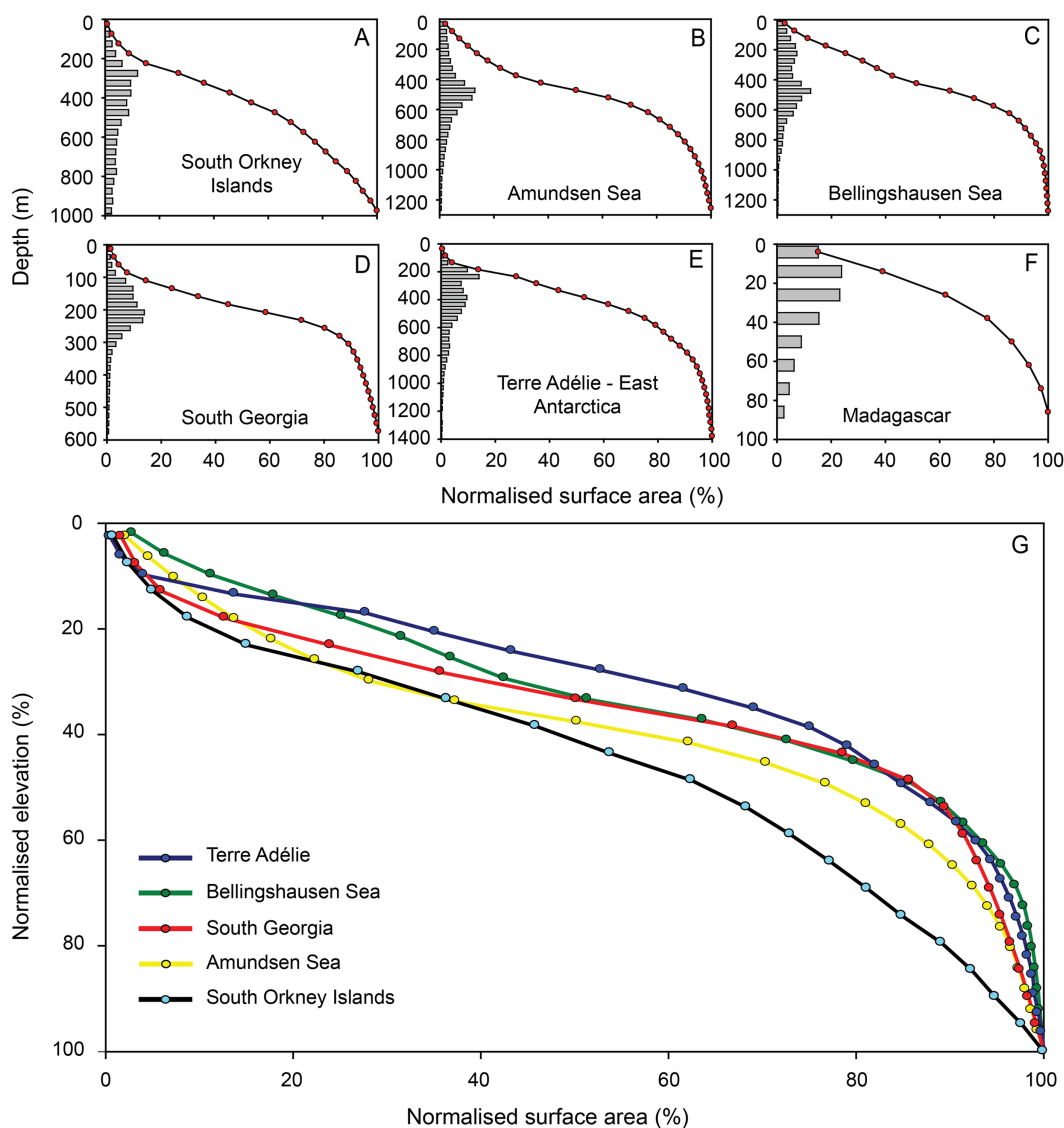


Figure 10. Hypsometric analysis of (a) the South Orkney continental shelf, (b) the Amundsen [Nitsche et al., 2007], and (c) Bellingshausen Seas [Graham et al., 2011]; (d) South Georgia [Graham et al., 2008], (e) Terre Adélie Land [Beaman et al., 2011], and (f) Madagascar [GEBCO, 2008]. Plots (a–f) display elevation histograms and cumulative depth curves. Plot (g) displays the normalized elevation versus normalized surface area for all the Antarctic bathymetric grids. Locations for each of the bathymetric grids are displayed in Figure 1.

the Laptev and East Siberian Sea, which are thought to have a less extensive glacial history [Kleiber and Nielsen, 1999], exhibited the same, convex upward profile. Given these observations, it seems likely that the differences in hypsometric curves are driven by the influence of former ice sheets that inhabited these shelves [cf. Jakobsson, 2002]. Thus, the hypsometric analysis displayed in Figures 10a–10f indicates similarity between the South Orkney shelf and that of other, formerly glaciated shelves in both the Arctic and Antarctic.

The mechanism that produces these distinct hypsometric profiles is probably a lowering of surface elevation, caused by the removal of substrate through the erosive action of large ice masses. This lowering will be most pronounced in the large, cross-shelf trough systems. Thus, the erosion and subsequent lowering will focus surface area in a particular depth range. When plotted on a normalized scale, this range is probably a function of the trough depths and that of the intervening shallow banks.

A diverse range of factors influences a hypsometric curve (e.g., structural geology, sediment deposition, and slope failures), making it difficult to establish a single control. However, by normalizing the hypsometric

profiles for the South Orkney shelf and additional Antarctic shelves (Figure 10g), a more detailed comparison is possible. If the distinct profile curves of glaciated shelves reflect lowering from glacial erosion, then we can assume that curves with a low gradient (i.e., more surface area in a limited depth range) reflect shelves that are more influenced by glacial erosion. Conversely, curves with less surface area within a limited depth range may reflect shelves where glacial erosion is less pervasive.

Normalized hypsometry of the Bellingshausen and Amundsen Seas, South Georgia and Terre Adélie Land reveals that, as a broad rule, these shelves have ~70% of their surface area within a ~30% elevation range (this elevation range is slightly larger for the Amundsen Sea). The tail of these curves shows a steep drop off, suggesting that the surface lowering is widespread across the shelf, possibly up to the shelf edge. Geophysical studies have shown this to be true—deep cross-shelf troughs have been identified in each region which extend to the shelf edge [Ó Cofaigh *et al.*, 2005b; Nitsche *et al.*, 2007; Graham *et al.*, 2008; Beaman *et al.*, 2011]. In contrast, the South Orkney hypsometric curve does not exhibit such a pronounced focusing of surface area. In fact, just ~50% of surface area is in the 30% range. In addition, the steep tail is absent and, with an even distribution of surface area at greater depths, the curve exhibits characteristics more similar to non-glaciated basin such as Madagascar (Figure 10f). Thus, hypsometry of the South Orkney shelf suggests that glacial erosion was less extensive and possibly restricted to shallow water depths; the deeper regions appear unaffected by glacial erosion. This interpretation is consistent with the limited extent of glaciations on the southern shelf, inferred from the mid-shelf break. Thus, as a working hypothesis, the difference between the South Orkney shelf and shelves elsewhere in Antarctica, revealed by the hypsometric analysis, is related to less frequent and/or less extensive glaciations on the southern continental shelf. However, we recognise the sensitivity of hypsometry to changes in shelf edge extent, and additional echosounding data are required to better constrain the continental shelf region.

The observation that South Georgia exhibits a similar curve to basins in Antarctica, despite its maritime, sub-polar climate, at first appears anomalous. However, we believe this is explained by the large proportion of continental shelf that is above sea level and thus available for ice accumulation, in addition to the relatively shallow continental shelf. Together, these factors will have enabled grounded ice to extend to the shelf edge. Given that the hypsometric curves are normalized, the similarities between South Georgia and the Antarctic basins reflect the shelf edge extent of glaciations in each respective region.

5. Discussion

5.1. Palaeo-Ice Sheet Drainage and Shelf Evolution

The new bathymetric compilation provides greater detail and improved insight into the geological structure and glacial development of the South Orkney continental shelf. It reveals a sea floor strongly influenced by glacial activity and suggests that the development of the continental shelf has been subject to significant glacial erosion and deposition. The shelf is dominated by seven deeply incised trough systems which indicate the presence of widespread grounded ice on the shelf in the past. The troughs would have focused ice flow, concentrating erosion on the shelf, while intervening shallow banks probably supported slower moving ice.

Based on their morphology (U-shaped, steep-walled, broad, and deep), Monroe and Coronation Troughs reflect well defined, deeply incised drainage pathways and indicate that ice was grounded at the northern shelf edge at some time in the past. Although poorly imaged, it is likely that ice occupied Powell, Laurie and Bennett Troughs and also extended to the shelf edge. In contrast, Signy and Orwell Troughs appear less deeply incised, weakly defined glacial pathways. They indicate that ice was not grounded at the shelf edge in the south. A lack of troughs directly north of the islands may result from the sparse coverage of depth soundings, or it may imply that during past ice cap advances ice preferentially flowed southward.

5.1.1. Regional Trough Asymmetry

A marked asymmetry exists between troughs in the north-west and in the south. The morphology of Monroe and Coronation troughs (U-shaped, steep sided, ~600–800 m deep) is significantly different to the morphology of Signy and Orwell troughs (broadly U-shaped, less steep sided and <400 m deep). When compared to troughs on the Antarctic mainland, the depth-width ratios of Monroe and Coronation Troughs (0.09 and 0.085 respectively) are extraordinary. For comparison, the depth-width ratio of Belgica Trough, Bellingshausen Sea, is 0.006 [Graham *et al.*, 2011], and Halley Trough, Weddell Sea, has a ratio of 0.009

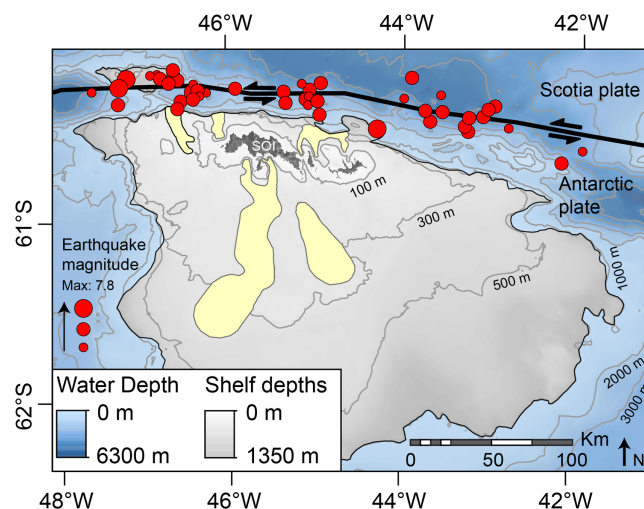


Figure 11. Earthquake locations between 19 October 2013 and 19 November 2013, from by the USGS. Larger red circles represent earthquakes of greater magnitude.

[Gales *et al.*, 2014]. Thus, the depth-width ratios of Monroe and Coronation Troughs are an order of magnitude greater than other Antarctic Troughs.

One possible explanation for the asymmetry is that ice flowing north of the South Orkney Islands was able to exploit tectonic structures that formed close to the South Scotia Ridge. Indeed, recent earthquake activity (Figure 11) illustrates that seismic activity is focused along the northern margin in a series of clusters. Notable clusters occur close to Monroe and Orwell Troughs, as well as Powell and Laurie Troughs. Importantly, no activity was measured south of the islands.

These clusters may reveal regions of greater stress release, and therefore probably greater prior stress accumulation, between the Scotia and Antarctic plates along the lateral (sinistral) transform margin. The stresses produced at these locations are likely to propagate into the plates on either side of the boundary, resulting in the formation of faults. Geological investigations into regions around Antarctica have shown that former ice sheets have exploited similar weak, structural faults, and tectonic lineaments, encouraging the formation of large cross-shelf troughs [Gohl, 2012]. Dynamic behavior in modern-day Antarctic ice streams is also thought to be influenced strongly by geological structures aligned with cross-shelf troughs [Bingham *et al.*, 2012]. The potential for recently active faults north of the South Orkney Islands, and their possible absence, or reduced significance, on the southern shelf, may explain the distinct asymmetry in trough morphology. Fast flowing ice in the north could have preferentially eroded the structurally weak continental shelf, producing the deep, steep sided trough systems. In contrast, ice flowing south of the islands may not have encountered similar structurally weak shelf substrate. This mechanism would also explain the extraordinary morphology in relation to troughs on the Antarctic shelf.

5.2. Age of the Glacial Troughs

Given the depth of incision and size, it is unlikely that the trough systems documented in this study were formed during the Last Glacial Maximum (LGM) alone. They were most likely carved through repeated glacial cycles, when each ice cap advance accentuated the existing drainage pathways. The South Orkney Islands have been a tectonically stable site for glaciation for around ~20 million years [King and Barker, 1988; Coren *et al.*, 1997]. On the Antarctic Peninsula mainland, mountain glaciation was initiated as early as 37–34 Ma [see Anderson *et al.*, 2011] while nearby drilling results (ODP Leg 113 Site 696) suggest intermittent glaciation of the South Orkney shelf with little sea ice during most of the Miocene and a persistent ice cap to sea-level on West Antarctica since the late Miocene to present [Kennett and Barker, 1990]. King *et al.* [1997] identified two seismic units in the nearby Powell Basin which they interpreted to record the onset of glacial-interglacial cyclicity and specifically the supply of ice-rafted debris to the basin in the late Miocene. Thus, it is likely that the troughs have been formed over several million years—certainly since the late Miocene and possibly even earlier—and were potentially last occupied during the LGM [e.g., Herron and Anderson, 1990].

5.3. Maximum Extent of Grounded Ice

Herron and Anderson [1990] place the maximum Quaternary grounding line advance around the South Orkney Islands at the 250–300 m isobath, and consider open marine conditions to have existed over the SOM since c. 9442–13848 cal kyr BP (although this has been previously been reported as 6000–7000 cal kyr BP in previous reviews; see Hodgson *et al.* [2014], for further discussion). Although the precise timing of Quaternary glacial advances and retreats is uncertain, the large, plateau-wide, mid-shelf glacial depocenter represents a

significant new finding. It represents a remarkable, time independent constraint on former grounding line margins across the entire South Orkney shelf. As with the troughs, the lack of current age data means that it remains unclear if the feature represents the terminal limit of several ancient (pre-LGM), or relatively recent (LGM) grounded ice advances, or a temporary limit formed during post-LGM ice retreat. It is commonly assumed that grounded ice extended to the shelf edge along much of the Antarctic continental shelf during the LGM, e.g., Antarctic Peninsula [Canals *et al.*, 2002; Ó Cofaigh *et al.*, 2002; Evans *et al.*, 2005; Heroy and Anderson, 2005; Ó Cofaigh *et al.*, 2005a; Domack *et al.*, 2006; Graham and Smith, 2012], the Amundsen and Bellingshausen Seas [Wellner *et al.*, 2001; Lowe and Anderson, 2002; Ó Cofaigh *et al.*, 2005b; Graham *et al.*, 2010; Hillenbrand *et al.*, 2010; Smith *et al.*, 2011], and the sub-Antarctic [Graham *et al.*, 2008]. However, notable exceptions occur in Prydz Bay, East Antarctica, and the western Ross Sea, where large-scale depositional features (grounding zone wedges) are thought to represent the terminal limit of grounded ice during the LGM [Domack *et al.*, 1998, 1999; O'Brien *et al.*, 1999; Shipp *et al.*, 1999; O'Brien *et al.*, 2007].

The absence of any clear sea-floor landforms (e.g., troughs or marginally formed geomorphic landforms) seaward of the mid-shelf break in the South Orkney data set suggests that, regardless of age, grounded ice did not extend beyond this point, at least during late Quaternary glacial episodes. The absence of any erosional unconformities at shallow sub-sea-floor depths beyond the feature on seismic line BAS845-16 supports this hypothesis. Furthermore, ODP Leg 113 Site 696, which was drilled at a location seaward of the depocenter (Figure 1b) recovered a sedimentary sequence of Quaternary age that consists of an olive/olive gray diatom-bearing silty mud [Barker *et al.*, 1988] without any evidence of grounded ice. Similarly, a set of gravity cores collected seaward of the mid-shelf break on the SE part of the shelf recovered Quaternary to Late Pliocene glaciomarine sediments but no subglacial deposits [Pudsey *et al.*, 1987]. Thus, the continent wide grounding zone margin is interpreted as the maximum limit of Quaternary glaciations on the South Orkney continental shelf.

This conclusion is also supported by (i) the shelf hypsometry which suggests a spatially restricted glacial influence, and (ii) the overall profile of the outer shelf south of the islands, which gently rolls away into deeper water. Extensive E-W and NNW-SSE trending extension faults, formed before and after the Oligocene separation of the SOM from the Antarctic Peninsula thinned the continental crust on the southern shelf [King and Barker, 1988]. Due to isostasy, lithosphere bearing thinner crust sits at an increased depth, where it floats on the underlying asthenosphere; this produces the greater water depths observed on the southern shelf when compared to the north. Unlike other parts of the Antarctic margin where grounded ice extended to the shelf edge during previous glacial maxima, the South Orkney ice cap may not have reached the southern shelf edge because glaciers could not become thick enough at their margins in order to ground. It is unlikely that the terrestrial catchment area would ever have been large enough to support such a huge volume of marine-based ice. The finding of a former limit is thus a realistic constraint on former glacial maxima.

The depth of this glacial limit, which is approximated with the ~300–350 m contour, is broadly consistent with findings from earlier geological investigations [Sugden and Clapperton, 1977; Herron and Anderson, 1990]. However, the new, high resolution bathymetry has enabled us to define this limit across the entire shelf. Despite this, the determination of the nature, number, and timing of the grounding event(s) requires verification with additional geological and seismic information.

5.4. Preliminary Ice Cap Reconstruction

Based on the above interpretations, and using data from the new bathymetric grid, we are able to propose a new reconstruction of the South Orkney ice cap during maximum glaciations (Figure 12). This reconstruction is time-independent but most likely represents a maximum Quaternary glacial scenario, and provides a model that can be tested in future studies.

Under Last Glacial Maximum conditions, global sea level would have been ~120 m lower than it is today, exposing a larger area of continental shelf above sea level (~2600 km², Figure 12) [Clark and Mix, 2002; Lambeck *et al.*, 2002] (N.B. the global sea level change is used as a simplified estimate of relative sea fall in this region, and does not take into account any local depression as a result of glacial isostatic loading). Thus, compared to the modern day, a significantly greater area for ice accumulation would have existed. Major outlets, potentially in the form of fast flowing ice streams or outlet glaciers, would have drained an expanded ice cap centered on and around the South Orkney Islands. These outlets are much narrower than those on the Antarctic Peninsula and even South Georgia [Ó Cofaigh *et al.*, 2002; Domack *et al.*, 2006;

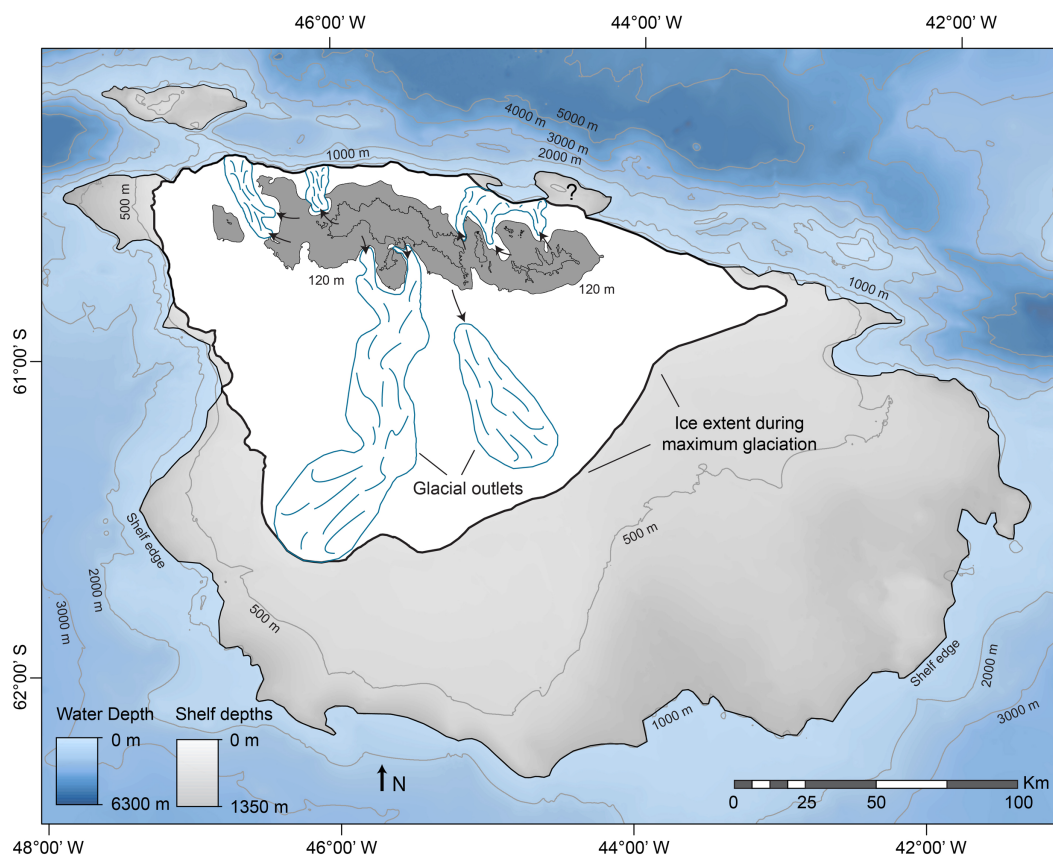


Figure 12. Ice cap reconstruction for the South Orkney continental shelf during maximum glaciations. The area above the modern 120 m water depth contour, shaded in dark grey, illustrates the reconstructed terrestrial part of the ice cap during maximum glacial conditions, while the black line within delineates the modern shoreline. The white regions represent areas of slower moving, possibly cold-based ice, while the regions with blue lines represent faster moving, more erosive ice. The arrows mark potential drainage routes from a former ice cap that would have been centered on and around the islands.

[Graham *et al.*, 2008; Graham and Smith, 2012]. Assuming similar flow velocity rates, and in spite of the depths that the northern troughs reach, this scenario may suggest that volumes of ice discharge through the South Orkney cross-shelf troughs were lower than in their Antarctic counterparts, although further computer modeling is required to clarify this. The glacial troughs initiate at some distance from the coastline, though in each case (excluding Orwell Trough) the onset zones appear to closely coincide with the -120 m contour, indicating that sea level had a pronounced influence on ice dynamics.

The mid-shelf glacial depocenter, interpreted as the terminal limit for grounded ice, can be traced across most of the continental shelf, providing a precise constraint on ice sheet extent. Using this limit, the estimated area of an ice cap during maximum glaciation is $\sim 19,000$ km²; that is more than four times the size of the modern day Academy of Sciences Ice Cap in the Russian Arctic and about 1.5 times the size of Devon Ice Cap, Arctic Canada [Dowdeswell *et al.*, 2002, 2004]. This size is considerably smaller than that of the Antarctic ice sheets but is analogous to that of the reconstructed palaeo-ice cap on South Georgia, which could have covered an area of $\sim 50,000$ km², assuming grounded ice extended to the shelf edge [Graham *et al.*, 2008].

6. Summary

1. We have produced a new bathymetric compilation (Figure 4), with a grid resolution of 300 m that offers significant improvements over previous grids of the South Orkney Islands continental shelf and slope.
2. The grid serves as a baseline product for scientific communities engaged in research around the Antarctic Peninsula and subpolar islands. It will have utility in oceanographic science (e.g., evaluating pathways for water masses), biological investigations (e.g., ecology and habitat mapping) as well as geological and glaciological studies.

3. The bathymetry reveals a continental shelf shaped predominantly by former glacial activity. A series of large and deep cross-shelf troughs would have acted as the major drainage pathway from an ice cap centered on the islands. Intervening shallow banks may have supported slowly moving, perhaps even cold based ice.
4. A continent wide glacial sediment depocenter, identified from seismic-reflection data (Figure 9) and visualized for the first time using the new bathymetry (Figures 4 and 8), is interpreted as the limit of grounded ice on the continental shelf during glacial maxima.
5. The South Orkney continental shelf hosted an ice cap with an area of $\sim 19,000$ km² during maximum glaciations (Figure 12). This size is smaller but roughly comparable to past ice sheet extent on nearby South Georgia.

Acknowledgments

We would like to thank Richard Gyllencreutz and two anonymous reviewers for their comments which greatly improved the clarity of our arguments. We would also like to thank the captains, crew, and scientists of all research vessels involved in data collection for this work. We also thank Ole Hestvik for the contribution of Olex data and Povl Abrahamsen for his collection and processing of swath multibeam data in the Scotia Ridge sector. This study is part of the British Antarctic Survey Polar Science for Planet Earth Programme. It was funded by the Natural Environment Research Council [NE/K50094X/1]. The full bathymetric grid is available through the Integrated Earth Data Applications (IEDA) Marine Geoscience Data System (MGDS): http://www.marine-geo.org/tools/search/Files.php?data_set_uid=21397.

References

- Anderson, J. B., et al. (2011), Progressive Cenozoic cooling and the demise of Antarctica's last refugium, *Proc. Natl. Acad. Sci. U. S. A.*, *108*(28), 11,356–11,360, doi:10.1073/pnas.1014885108.
- Arndt, J. E., et al. (2013), The International Bathymetric Chart of the Southern Ocean (IBCSO) Version 1.0: A new bathymetric compilation covering circum-Antarctic waters, *Geophys. Res. Lett.*, *40*, 3111–3117, doi:10.1002/grl.50413.
- Barker, P. F., et al. (1988), Preliminary results of ODP Leg-113 of Joides-Resolution in the Weddell Sea: History of the Antarctic Glaciation, *C. R. Acad. Sci., Ser. I*, *306*(1), 73–78.
- Beaman, R. J., P. E. O'Brien, A. L. Post, and L. De Santis (2011), A new high-resolution bathymetry model for the Terre Adelie and George V continental margin, East Antarctica, *Antarct. Sci.*, *23*(1), 95–103, doi:10.1017/S095410201000074x.
- Bentley, M. J., and J. B. Anderson (1998), Glacial and marine geological evidence for the ice sheet configuration in the Weddell Sea Antarctic Peninsula region during the Last Glacial Maximum, *Antarct. Sci.*, *10*(3), 309–325.
- Bingham, R. G., F. Ferraccioli, E. C. King, R. D. Larter, H. D. Pritchard, A. M. Smith, and D. G. Vaughan (2012), Inland thinning of West Antarctic Ice Sheet steered along subglacial rifts, *Nature*, *487*(7408), 468–471, doi:10.1038/nature11292.
- Bradwell, T., et al. (2008), The northern sector of the last British Ice Sheet: Maximum extent and demise, *Earth Sci. Rev.*, *88*(3–4), 207–226, doi:10.1016/j.earscirev.2008.01.008.
- Brocklehurst, S. H., and K. X. Whipple (2002), Glacial erosion and relief production in the Eastern Sierra Nevada, California, *Geomorphology*, *42*(1–2), 1–24, doi:10.1016/S0169-555x(01)00069-1.
- Burns, J. M., D. P. Costa, M. A. Fedak, M. A. Hindell, C. J. A. Bradshaw, N. J. Gales, B. McDonald, S. J. Trumble, and D. E. Crocker (2004), Winter habitat use and foraging behavior of crabeater seals along the Western Antarctic Peninsula, *Deep Sea Res., Part I*, *51*(17–19), 2279–2303, doi:10.1016/j.dsr.2.2004.07.021.
- Canals, M., J. L. Casamor, R. Urgeles, A. M. Calafat, E. W. Domack, J. Baraza, M. Farran, and M. De Batist (2002), Seafloor evidence of a subglacial sedimentary system off the northern Antarctic Peninsula, *Geology*, *30*(7), 603–606, doi:10.1130/0091-7613(2002)030<0603:Seoass>2.0.Co;2.
- Caress, D. W., and D. N. Chayes (1996), Improved processing of Hydrosweep DS multibeam data on the R/V Maurice Ewing, *Mar. Geophys. Res.*, *18*(6), 631–650, doi:10.1007/BF00313878.
- CCAMLR (2005), *Report of the 24th Meeting of the Commission*, Hobart, Australia.
- Civile, D., E. Lodolo, A. Vuan, and M. F. Loreto (2012), Tectonics of the Scotia-Antarctica plate boundary constrained from seismic and seismological data, *Tectonophysics*, *550*, 17–34, doi:10.1016/j.tecto.2012.05.002.
- Clark, P. U., and A. C. Mix (2002), Ice sheets and sea level of the Last Glacial Maximum, *Quat. Sci. Rev.*, *21*(1–3), 1–7, doi:10.1016/S0277-3791(01)00118-4.
- Clarke, A., and R. J. G. Leakey (1996), The seasonal cycle of phytoplankton, macronutrients, and the microbial community in a nearshore Antarctic marine ecosystem, *Limnol. Oceanogr.*, *41*(6), 1281–1294.
- Coren, F., G. Ceccone, E. Lodolo, C. Zanolla, N. Zitellini, C. Bonazzi, and J. Centonze (1997), Morphology, seismic structure and tectonic development of the Powell Basin, Antarctica, *J. Geol. Soc. London*, *154*, 849–862, doi:10.1144/gsjgs.154.5.0849.
- Domack, E., P. O'Brien, P. Harris, F. Taylor, P. G. Quilty, L. De Santis, and B. Raker (1998), Late Quaternary sediment facies in Prydz Bay, East Antarctica and their relationship to glacial advance onto the continental shelf, *Antarct. Sci.*, *10*(3), 236–246.
- Domack, E., E. A. Jacobson, S. Shipp, and J. B. Anderson (1999), Late Pleistocene-Holocene retreat of the West Antarctic Ice-Sheet system in the Ross Sea. Part 2: Sedimentologic and stratigraphic signature, *Geol. Soc. Am. Bull.*, *111*(10), 1517–1536, doi:10.1130/0016-7606(1999)111<1517:iphrot>2.3.Co;2.
- Domack, E., D. Amblas, R. Gilbert, S. Brachfeld, A. Camerlenghi, M. Rebesco, M. Canals, and R. Urgeles (2006), Subglacial morphology and glacial evolution of the Palmer deep outlet system, Antarctic Peninsula, *Geomorphology*, *75*(1–2), 125–142, doi:10.1016/j.geomorph.2004.06.013.
- Dowdeswell, J. A., and A. Elverhoi (2002), The timing of initiation of fast-flowing ice streams during a glacial cycle inferred from glaciomarine sedimentation, *Mar. Geol.*, *188*(1–2), 3–14, doi:10.1016/S0025-3227(02)00272-4.
- Dowdeswell, J. A., and E. M. G. Fugelli (2012), The seismic architecture and geometry of grounding-zone wedges formed at the marine margins of past ice sheets, *Geol. Soc. Am. Bull.*, *124*(11–12), 1750–1761, doi:10.1130/B30628.1.
- Dowdeswell, J. A., and M. Vasquez (2013), Submarine landforms in the fjords of southern Chile: Implications for glaciomarine processes and sedimentation in a mild glacier-influenced environment, *Quat. Sci. Rev.*, *64*, 1–19, doi:10.1016/j.quascirev.2012.12.003.
- Dowdeswell, J. A., et al. (2002), Form and flow of the Academy of Sciences Ice Cap, Severnaya Zemlya, Russian High Arctic, *J. Geophys. Res.*, *107*(B4), 2076, doi:10.1029/2000JB000129.
- Dowdeswell, J. A., T. J. Benham, M. R. Gorman, D. Burgess, and M. J. Sharp (2004), Form and flow of the Devon Island Ice Cap, Canadian Arctic, *J. Geophys. Res.*, *109*, F02002, doi:10.1029/2003JF000095.
- Dowdeswell, J. A., D. Ottesen, and L. Rise (2010), Rates of sediment delivery from the Fennoscandian Ice Sheet through an ice age, *Geology*, *38*(1), 3–6, doi:10.1130/G25523.1.
- Dutrieux, P., J. De Rydt, A. Jenkins, P. R. Holland, H. K. Ha, S. H. Lee, E. J. Steig, Q. Ding, E. P. Abrahamsen, and M. Schröder (2014), Strong sensitivity of Pine Island ice-shelf melting to climatic variability, *Science*, *343*(6167), 174–178, doi:10.1126/science.1244341.

- Egholm, D. L., S. B. Nielsen, V. K. Pedersen, and J. E. Lesemann (2009), Glacial effects limiting mountain height, *Nature*, 460(7257), 884–U120, doi:10.1038/nature08263.
- Emery, K. O. (1979), Hypsometry of the continental-shelf off Eastern North-America, *Estuarine Coastal Shelf. Sci.*, 9(5), 653–658, doi:10.1016/0302-3524(79)90089-6.
- Evans, J., C. J. Pudsey, C. Ó Cofaigh, P. Morris, and E. Domack (2005), Late Quaternary glacial history, flow dynamics and sedimentation along the eastern margin of the Antarctic Peninsula Ice Sheet, *Quat. Sci. Rev.*, 24(5–6), 741–774, doi:10.1016/j.quascirev.2004.10.007.
- Favero-Long, S. E., M. R. Worland, P. Convey, R. I. L. Smith, R. Piervittori, M. Guglielmin, and N. Cannone (2012), Primary succession of lichen and bryophyte communities following glacial recession on Signy Island, South Orkney Islands, Maritime Antarctic, *Antarct. Sci.*, 24(4), 323–336, doi:10.1017/S0954102012000120.
- Flores, H., C. Haas, J. A. van Franeker, and E. Meesters (2008), Density of pack-ice seals and penguins in the western Weddell Sea in relation to ice thickness and ocean depth, *Deep Sea Res., Part I*, 55(8–9), 1068–1074, doi:10.1016/j.dsr.2007.12.024.
- Fretwell, P., et al. (2013), Bedmap2: Improved ice bed, surface and thickness datasets for Antarctica, *Cryosphere*, 7(1), 375–393, doi:10.5194/tc-7-375-2013.
- GEBCO (2008), The GEBCO 08 Grid. [Available at <http://www.gebco.net/>].
- Gales, J. A., P. T. Leat, R. D. Larter, G. Kuhn, C.-D. Hillenbrand, A. G. C. Graham, N. C. Mitchell, A. J. Tate, G. B. Buys, and W. Jokat (2014), Large-scale submarine landslides, channel and gully systems on the southern Weddell Sea margin, *Antarctica, Marine Geology*, 348, 73–87, doi:10.1016/j.margeo.2013.12.002.
- Gohl, K. (2012), Basement control on past ice sheet dynamics in the Amundsen Sea Embayment, West Antarctica, *Palaeogeogr. Palaeoclimatol. Paleocool.*, 335, 35–41, doi:10.1016/j.palaeo.2011.02.022.
- Graham, A. G. C., and J. A. Smith (2012), Palaeoglaciology of the Alexander Island ice cap, western Antarctic Peninsula, reconstructed from marine geophysical and core data, *Quat. Sci. Rev.*, 35, 63–81, doi:10.1016/j.quascirev.2012.01.008.
- Graham, A. G. C., P. T. Fretwell, R. D. Larter, D. A. Hodgson, C. K. Wilson, A. J. Tate, and P. Morris (2008), A new bathymetric compilation highlighting extensive paleo-ice sheet drainage on the continental shelf, South Georgia, sub-Antarctica, *Geochem. Geophys. Geosyst.*, 9, Q07011, doi:10.1029/2008GC001993.
- Graham, A. G. C., R. D. Larter, K. Gohl, J. A. Dowdeswell, C. D. Hillenbrand, J. A. Smith, J. Evans, G. Kuhn, and T. Deen (2010), Flow and retreat of the Late Quaternary Pine Island-Thwaites palaeo-ice stream, West Antarctica, *J. Geophys. Res.*, 115, F03025, doi:10.1029/2009JF001482.
- Graham, A. G. C., F. O. Nitsche, and R. D. Larter (2011), An improved bathymetry compilation for the Bellingshausen Sea, Antarctica, to inform ice-sheet and ocean models, *Cryosphere*, 5(1), 95–106, doi:10.5194/tc-5-95-2011.
- Griffiths, S. D., and W. R. Peltier (2009), Modeling of polar ocean tides at the last glacial maximum: Amplification, sensitivity, and climatological implications, *J. Clim.*, 22(11), 2905–2924, doi:10.1175/2008jcli2540.1.
- Hellmer, H. H., F. Kauker, R. Timmermann, J. Determann, and J. Rae (2012), Twenty-first-century warming of a large Antarctic ice-shelf cavity by a redirected coastal current, *Nature*, 485(7397), 225–228, doi:10.1038/nature11064.
- Heroy, D. C., and J. B. Anderson (2005), Ice-sheet extent of the Antarctic Peninsula region during the Last Glacial Maximum (LGM): Insights from glacial geomorphology, *Geol. Soc. Am. Bull.*, 117(11–12), 1497–1512, doi:10.1130/B25694.1.
- Herron, M. J., and J. B. Anderson (1990), Late quaternary glacial history of the South Orkney Plateau, Antarctica, *Quat. Res.*, 33(3), 265–275, doi:10.1016/0033-5894(90)90055-P.
- Hillenbrand, C. D., R. D. Larter, J. A. Dowdeswell, W. Ehrmann, C. O. Cofaigh, S. Benetti, C. Ó Cofaigh, and H. Grobe (2010), The sedimentary legacy of a palaeo-ice stream on the shelf of the southern Bellingshausen Sea: Clues to West Antarctic glacial history during the Late Quaternary, *Quat. Sci. Rev.*, 29(19–20), 2741–2763, doi:10.1016/j.quascirev.2010.06.028.
- Hodgson, D. A., et al. (2014), Terrestrial and submarine evidence for the extent and timing of the Last Glacial Maximum and the onset of deglaciation on the maritime-Antarctic and sub-Antarctic islands, *Quat. Sci. Rev.*, in press.
- Holt, J. W., D. D. Blankenship, D. L. Morse, D. A. Young, M. E. Peters, S. D. Kempf, T. G. Richter, D. G. Vaughan, and H. F. J. Corr (2006), New boundary conditions for the West Antarctic Ice Sheet: Subglacial topography of the Thwaites and Smith glacier catchments, *Geophys. Res. Lett.*, 33, L09502, doi:10.1029/2005GL025561.
- Hutchinson, M. F. (1988), Calculation of hydrologically sound digital elevation models, paper presented at Third International Symposium on Spatial Data Handling, Sydney.
- Hutchinson, M. F. (1989), A new procedure for gridding elevation and stream line data with automatic removal of spurious pits, *J. Hydrol.*, 106, 211–232.
- Hutchinson, M., T. Xu, and J. Stein (2011), Recent Progress in the ANUDEM Elevation Gridding Procedure, ESRI, *Geomorphology 2011, Geomorphometry.org, Online*, pp. 19–22.
- Jakobsson, M. (2002), Hypsometry and volume of the Arctic Ocean and its constituent seas, *Geochem. Geophys. Geosyst.*, 3(5), 1028, doi:10.1029/2001GC000302.
- Jakobsson, M., L. Polyak, M. Edwards, J. Kleman, and B. Coakley (2008), Glacial geomorphology of the Central Arctic Ocean: The Chukchi Borderland and the Lomonosov Ridge, *Earth Surf. Processes Landforms*, 33(4), 526–545, doi:10.1002/esp.1667.
- Jakobsson, M., J. B. Anderson, F. O. Nitsche, R. Gyllencreutz, A. E. Kirshner, N. Kirchner, M. O'Regan, R. Mohammad, and B. Eriksson (2012), Ice sheet retreat dynamics inferred from glacial morphology of the central Pine Island Bay Trough, West Antarctica, *Quat. Sci. Rev.*, 38, 1–10, doi:10.1016/j.quascirev.2011.12.017.
- Kennett, J. P., and P. F. Barker (1990), Latest Cretaceous to Cenozoic climate and oceanographic developments in the Weddell Sea, Antarctica: An ocean-drilling perspective, in *Proceedings of the Ocean Drilling Program, Scientific Results*, vol. 113, edited by P. F. Barker and J. P. Kennett et al., pp. 937–960, Ocean Drilling Program, College Station, Tex.
- King, E. C., and P. F. Barker (1988), The margins of the South Orkney microcontinent, *J. Geol. Soc. London*, 145, 317–331, doi:10.1144/gsjgs.145.2.0317.
- King, E. C., G. Leitchenkov, J. Galindo-Zaldivar, A. Maldonado, and E. Lodolo (1997), Crustal structure and sedimentation in Powell Basin, in *Geology and Stratigraphy of the Antarctic Margin Part 2, Antarct. Res. Ser.*, vol. 71, edited by P. F. Barker and A. K. Cooper, pp. 75–93, AGU, Washington, D. C.
- Klages, J. P., G. Kuhn, C. D. Hillenbrand, A. G. C. Graham, J. A. Smith, R. D. Larter, and K. Gohl (2013), First geomorphological record and glacial history of an inter-ice stream ridge on the West Antarctic continental shelf, *Quat. Sci. Rev.*, 61, 47–61, doi:10.1016/j.quascirev.2012.11.007.
- Kleiber, H. P., and F. Niessen (1999), Late Pleistocene paleoriver channels on the Laptev Sea Shelf: Implications from sub-bottom profiling, in *Land-Ocean Systems in the Siberian Arctic*, edited by H. Kassens, et al., pp. 657–665, Springer, Berlin.
- Lambeck, K., Y. Yokoyama, and T. Purcell (2002), Into and out of the last glacial maximum: Sea-level change during Oxygen Isotope Stages 3 and 2, *Quat. Sci. Rev.*, 21(1–3), 343–360, doi:10.1016/S0277-3791(01)00071-3.

- Larter, R. D., A. G. C. Graham, C. D. Hillenbrand, J. A. Smith, and J. A. Gales (2012), Late Quaternary grounded ice extent in the Filchner Trough, Weddell Sea, Antarctica: New marine geophysical evidence, *Quat. Sci. Rev.*, *53*, 111–122, doi:10.1016/j.quascirev.2012.08.006.
- Leat, P. T., A. J. Tate, D. R. Tappin, S. J. Day, and M. J. Owen (2010), Growth and mass wasting of volcanic centers in the northern South Sandwich arc, South Atlantic, revealed by new multibeam mapping, *Mar. Geol.*, *275*(1–4), 110–126, doi:10.1016/j.margeo.2010.05.001.
- Livingstone, S. J., C. Ó Cofaigh, C. R. Stokes, C. D. Hillenbrand, A. Vieli, and S. S. R. Jamieson (2012), Antarctic palaeo-ice streams, *Earth Sci. Rev.*, *111*(1–2), 90–128, doi:10.1016/j.earscirev.2011.10.003.
- Lowe, A. L., and J. B. Anderson (2002), Reconstruction of the West Antarctic Ice Sheet in Pine Island Bay during the last glacial maximum and its subsequent retreat history, *Quat. Sci. Rev.*, *21*(16–17), 1879–1897, doi:10.1016/S0277-3791(02)00006-9.
- Makinson, K., P. R. Holland, A. Jenkins, K. W. Nicholls, and D. M. Holland (2011), Influence of tides on melting and freezing beneath Filchner-Ronne Ice Shelf, Antarctica, *Geophys. Res. Lett.*, *38*, L06601, doi:10.1029/2010GL046462.
- Mayer, L. A., M. Paton, L. Gee, J. V. Gardner, and C. Ware (2000), Interactive 3-D visualization: A tool for seafloor navigation, exploration and engineering, in *Conference Proceedings on Oceans 2000 Mts/IEEE: Where Marine Science and Technology Meet*, vols. 1–3, pp. 913–919, IEEE, Providence, Rhode Island, USA.
- McConnell, B. J., C. Chambers, and M. A. Fedak (1992), Foraging ecology of southern elephant seals in relation to the bathymetry and productivity of the Southern Ocean, *Antarct. Sci.*, *4*(4), 393–398.
- McMullen, K., E. Domack, A. Leventer, C. Olson, R. Dunbar, and S. Brachfeld (2006), Glacial morphology and sediment formation in the Mertz Trough, East Antarctica, *Palaeogeogr. Palaeoclimatol. Palaeoecol.*, *231*(1–2), 169–180, doi:10.1016/j.palaeo.2005.08.004.
- Meredith, M. P., K. W. Nicholls, I. A. Renfrew, L. Boehme, M. Biuw, and M. Fedak (2011), Seasonal evolution of the upper-ocean adjacent to the South Orkney Islands, Southern Ocean: Results from a “lazy biological mooring,” *Deep Sea Res., Part I*, *58*(13–16), 1569–1579, doi:10.1016/j.dsr2.2009.07.008.
- Montgomery, D. R. (2002), Valley formation by fluvial and glacial erosion, *Geology*, *30*(11), 1047–1050, doi:10.1130/0091-7613(2002)030<1047:Vfbfag>2.0.Co;2.
- Murphy, E. J., A. Clarke, C. Symon, and J. Priddle (1995), Temporal variation in antarctic sea-ice: Analysis of a long-term fast-ice record from the South-Orkney Islands, *Deep Sea Res. Part I*, *42*(7), 1045–1062, doi:10.1016/0967-0637(95)00057-D.
- Murphy, E. J., P. N. Trathan, I. Everson, G. Parkes, and F. Daunt (1997), Krill fishing in the Scotia Sea in relation to bathymetry, including the detailed distribution around South Georgia, *CCAMLR Sci.*, *4*, 1–17.
- Nicholls, K. W., S. Osterhus, K. Makinson, T. Gammelsrod, and E. Fahrbach (2009), Ice-ocean processes over the continental shelf of the Southern Weddell Sea, Antarctica: A review, *Rev. Geophys.*, *47*, RG3003, doi:10.1029/2007RG000250.
- Nitsche, F. O., S. S. Jacobs, R. D. Larter, and K. Gohl (2007), Bathymetry of the Amundsen Sea continental shelf: Implications for geology, oceanography, and glaciology, *Geochem. Geophys. Geosyst.*, *8*, Q10009, doi:10.1029/2007GC001694.
- O’Brien, P. E., L. De Santis, P. T. Harris, E. Domack, and P. G. Quilty (1999), Ice shelf grounding zone features of western Prydz Bay, Antarctica: Sedimentary processes from seismic and sidescan images, *Antarct. Sci.*, *11*(1), 78–91.
- O’Brien, P. E., I. Goodwin, C. F. Forsberg, A. K. Cooper, and J. Whitehead (2007), Late Neogene ice drainage changes in Prydz Bay, East Antarctica and the interaction of Antarctic ice sheet evolution and climate, *Palaeogeogr. Palaeoclimatol. Palaeoecol.*, *245*(3–4), 390–410, doi:10.1016/j.palaeo.2006.09.002.
- Ó Cofaigh, C., C. J. Pudsey, J. A. Dowdeswell, and P. Morris (2002), Evolution of subglacial bedforms along a paleo-ice stream, Antarctic Peninsula continental shelf, *Geophys. Res. Lett.*, *29*(8), 1199, doi:10.1029/2001GL014488.
- Ó Cofaigh, C., J. A. Dowdeswell, C. S. Allen, J. F. Hiemstra, C. J. Pudsey, J. Evans, and D. J. A. Evans (2005a), Flow dynamics and till genesis associated with a marine-based Antarctic palaeo-ice stream, *Quat. Sci. Rev.*, *24*(5–6), 709–740, doi:10.1016/j.quascirev.2004.10.006.
- Ó Cofaigh, C., R. D. Larter, J. A. Dowdeswell, C. D. Hillenbrand, C. J. Pudsey, J. Evans, and P. Morris (2005b), Flow of the West Antarctic Ice Sheet on the continental margin of the Bellingshausen Sea at the Last Glacial Maximum, *J. Geophys. Res.*, *110*, B11103, doi:10.1029/2005JB003619.
- Ó Cofaigh, C., et al. (2013), An extensive and dynamic ice sheet on the West Greenland shelf during the last glacial cycle, *Geology*, *41*(2), 219–222, doi:10.1130/G33759.1.
- Ottesen, D., and J. A. Dowdeswell (2009), An inter-ice-stream glaciated margin: Submarine landforms and a geomorphic model based on marine-geophysical data from Svalbard, *Geol. Soc. Am. Bull.*, *121*(11–12), 1647–1665, doi:10.1130/B26467.1.
- Ottesen, D., J. A. Dowdeswell, and L. Rise (2005), Submarine landforms and the reconstruction of fast-flowing ice streams within a large Quaternary ice sheet: The 2500-km-long Norwegian-Svalbard margin (57 degrees-80 degrees N), *Geol. Soc. Am. Bull.*, *117*(7–8), 1033–1050, doi:10.1130/B25577.1.
- Ottesen, D., J. A. Dowdeswell, J. Y. Landvik, and J. Mienert (2007), Dynamics of the Late Weichselian ice sheet on Svalbard inferred from high-resolution sea-floor morphology, *Boreas*, *36*(3), 286–306, doi:10.1080/03009480701210378.
- Padman, L., H. A. Fricker, R. Coleman, S. Howard, and L. Erofeeva (2002), A new tide model for the Antarctic ice shelves and seas, *Ann. Glaciol.*, *34*, 247–254, doi:10.3189/172756402781817752.
- Pedersen, V. K., and D. L. Egholm (2013), Glaciations in response to climate variations preconditioned by evolving topography, *Nature*, *493*(7431), 206–210, doi:10.1038/nature11786.
- Pritchard, H. D., S. R. M. Ligtenberg, H. A. Fricker, D. G. Vaughan, M. R. van den Broeke, and L. Padman (2012), Antarctic ice-sheet loss driven by basal melting of ice shelves, *Nature*, *484*(7395), 502–505, doi:10.1038/nature10968.
- Pudsey, C. J., J. W. Murray, and P. F. Ciesielski (1987), Late Pliocene to quaternary sedimentation on the South Orkney Shelf, *Br. Antarct. Surv. Bull.*, *77*, 81–97.
- Ribic, C. A., E. Chapman, W. R. Fraser, G. L. Lawson, and P. H. Wiebe (2008), Top predators in relation to bathymetry, ice and krill during austral winter in Marguerite Bay, Antarctica, *Deep Sea Res., Part I*, *55*(3–4), 485–499, doi:10.1016/j.dsr2.2007.11.006.
- Rogers, A. D., et al. (2012), The discovery of new deep-sea hydrothermal vent communities in the southern ocean and implications for biogeography, *PLoS Biol.*, *10*(1), e1001234, doi:10.1371/journal.pbio.1001234.
- Rosier, S. H. R., J. A. M. Green, J. D. Scourse, and R. Winkelmann (2014), Modeling Antarctic tides in response to ice shelf thinning and retreat, *J. Geophys. Res.*, *119*, 87–97, doi:10.1002/2013JC009240.
- Shipp, S., J. Anderson, and E. Domack (1999), Late Pleistocene-Holocene retreat of the West Antarctic Ice-Sheet system in the Ross Sea. Part 1: Geophysical results, *Geol. Soc. Am. Bull.*, *111*(10), 1486–1516, doi:10.1130/0016-7606(1999)111<1486:jphrot>2.3.Co;2.
- Smalley, R., M. G. Bevis, A. F. Zakrajsek, F. N. Teferle, I. W. D. Dalziel, L. A. Lawver, and R. D. Larter (2013), Near field dynamic, co-seismic and post-seismic deformations associated with the 2013, M7.8, and 2003, M 7.6, *South Scotia Ridge earthquakes observed with GPS, Seismic Research Letters*, *85*(2), 490.
- Smith, J. A., C. D. Hillenbrand, G. Kuhn, R. D. Larter, A. G. C. Graham, W. Ehrmann, S. G. Moreton, and M. Forwick (2011), Deglacial history of the West Antarctic Ice Sheet in the western Amundsen Sea Embayment, *Quat. Sci. Rev.*, *30*(5–6), 488–505, doi:10.1016/j.quascirev.2010.11.020.

- Spotila, J. A., J. T. Buscher, A. J. Meigs, and P. W. Reiners (2004), Long-term glacial erosion of active mountain belts: Example of the Chugach St. Elias Range, Alaska, *Geology*, *32*(6), 501–504, doi:10.1130/G20343.1.
- Stewart, F. S., and M. S. Stoker (1990), Problems associated with seismic facies analysis of diamicton-dominated, shelf glacigenic sequences, *GeoMar. Lett.*, *10*(3), 151–156, doi:10.1007/BF02085930.
- Sugden, D. E., and C. M. Clapperton (1977), Maximum ice extent on island groups in Scotia Sea, Antarctica, *Quat. Res.*, *7*(2), 268–282, doi:10.1016/0033-5894(77)90041-2.
- Thoma, M., A. Jenkins, D. Holland, and S. Jacobs (2008), Modelling circumpolar deep water intrusions on the Amundsen Sea continental shelf, Antarctica, *Geophys. Res. Lett.*, *35*, L18602, doi:10.1029/2008GL034939.
- Thomas, C., R. Livermore, and F. Pollitz (2003), Motion of the Scotia Sea plates, *Geophys. J. Int.*, *155*(3), 789–804, doi:10.1111/j.1365-246X.2003.02069.x.
- Vaughan, D. G., G. J. Marshall, W. M. Connolley, C. Parkinson, R. Mulvaney, D. A. Hodgson, J. C. King, C. J. Pudsey, and J. Turner (2003), Recent rapid regional climate warming on the Antarctic Peninsula, *Clim. Change*, *60*(3), 243–274, doi:10.1023/A:1026021217991.
- Vaughan, D. G., H. F. J. Corr, F. Ferraccioli, N. Frearson, A. O'Hare, D. Mach, J. W. Holt, D. D. Blankenship, D. L. Morse, and D. A. Young (2006), New boundary conditions for the West Antarctic ice sheet: Subglacial topography beneath Pine Island Glacier, *Geophys. Res. Lett.*, *33*, L09501, doi:10.1029/2005GL025588.
- Walker, D. P., M. A. Brandon, A. Jenkins, J. T. Allen, J. A. Dowdeswell, and J. Evans (2007), Oceanic heat transport onto the Amundsen Sea shelf through a submarine glacial trough, *Geophys. Res. Lett.*, *34*, L02602, doi:10.1029/2006GL028154.
- Wellner, J. S., A. L. Lowe, S. S. Shipp, and J. B. Anderson (2001), Distribution of glacial geomorphic features on the Antarctic continental shelf and correlation with substrate: Implications for ice behavior, *J. Glaciol.*, *47*(158), 397–411, doi:10.3189/172756501781832043.